Technological Innovations for Mid-Atlantic Cropping Systems

Michael Swoish

Dissertation submitted to the faculty of the Virginia Polytechnic Institute and State University in partial fulfillment of the requirements for the degree of

Doctor of Philosophy
In
Crop and Soil Environmental Sciences

W. Thomason
M. Reiter
R. Stewart
J. Campbell

December 17, 2019
Blacksburg, VA

Keywords: Malt barley, plant growth regulator, trinexapac-ethyl, remote sensing, satellite imagery, spatial resolution, vegetation indices, cover crop biomass, indicator cop, phosphorus sensitive mutant, *Arabidopsis thaliana ipk1*$^{-}$

Technological Innovations for Mid-Atlantic Cropping Systems

Michael Swoish

ABSTRACT

Greater projected demand for food, fuel, and fiber will require substantial increases in global agricultural production over the next three decades. Climate change is also forecasted to make weather events more extreme and variable. Efficiency will become more important as demand for food products increases and the availability of fertilizer and land decreases. Technology may be of paramount importance for pushing the boundaries of production while remaining sustainable for generations to come. The first chapter of this dissertation investigated the importance of rate and timing of the plant growth regulator trinexapac-ethyl to malting barley in Virginia. Plant growth regulators can help plants remain upright during strong winds, thereby preserving grain quality and yield. However, this study demonstrated that risks of plant injury also exist. Application should be restricted to fields with greater risk of lodging and made only after the barley crop has broken dormancy and a substantial increase in air temperature is not forecasted in the week following application. Chapter two compared the efficacy of eight vegetation indices calculated from three satellites (Landsat 8, Sentinel 2, and Planet) for estimating cover crop biomass. Cover crops can have beneficial effects on agricultural land as well as groundwater and surface water, but only when adequate biomass is established to reduce erosion and nutrient leaching. Satellite imagery was able to estimate multi-species cover crop biomass more accurately than field-based sensors, although the most accurate vegetation index was dependent upon which satellite was being tested. Chapter three investigated the potential of *Arabidopsis thaliana ipk1*$^{-}$, a loss-of-function mutant which exhibits decreased growth at elevated phosphorus concentration, for serving as in indicator of plant available phosphorus. An indicator crop could provide greater spatial resolution compared to soil testing, as well as represent plant available nutrients as opposed to chemically extracted nutrient estimations. Plant response exhibited a quadratic relationship with media P concentration in the range of fertilizer decision making for maize, providing valuable insight for potential yield response in agricultural fields below 'very high' phosphorus concentration.

GENERAL AUDIENCE ABSTRACT

Climate change, increased demand for locally sourced ingredients, and elevated pressure for environmentally responsible practices will make meeting the growing demand for food difficult for farmers to achieve over the next few decades. Similar to many other industries, implementation of advanced technology may be necessary to keep up with agricultural demand. Plant growth regulators are one such technology which when applied to plants can cause them to remain short, decreasing the chance of blowing over during windstorms. However, chapter one of this dissertation concluded that risks of plant injury also exist when applying plant growth regulator on malting barley (for brewing or distilling). Application should be restricted to fields with greater risk of wind damage (e.g. taller barley) and made only after the barley crop begins spring growth and a decrease in air temperature is not forecasted in the week following application. Chapter two compared eight spectral vegetation indices across three satellites with different image resolution for their ability to estimate cover crop biomass. Cover crops protect groundwater and surface water quality, but only when adequate growth is achieved. Satellite imagery was able to estimate multi-species cover crop biomass more accurately than field-based sensors, although the most accurate vegetation index was dependent upon which satellite was being tested. Chapter three investigated the potential of *Arabidopsis thaliana ipk1*$^{-}$, a loss-of-function mutant which exhibits decreased growth at elevated phosphorus concentration, as in indicator of plant available phosphorus in soil. An indicator crop could help determine which areas of a field are likely to have increased crop yield if fertilized and which are not. The mutant tested could be useful as an

indicator crop given its response to phosphorus concentration, warranting further research with other plant species more appropriate for field use.

Contents

Introduction:

The global population is expected to reach 10 billion people in approximately 30 years, and experts have projected that the amount of food produced on an annual basis will need to double in order to meet consumption. Furthering the difficulty of meeting increased agricultural demand is the need to do so sustainably so that our soil, water, and fertilizer resources are not exhausted. The projects in this dissertation investigated ways in which technology may help ease the burden of producing more food on the same amount of land in the United States while protecting environmental quality. Improving upon current technologies and inventing new ones will be imperative for the needs of future generations.

A great deal of technology and research is already implemented in agricultural production in the US, but some of this technology may have untapped potential. Landsat 8 and Sentinel 2 satellite imagery can be downloaded without cost and is used across the world for many investigative purposes, but further utility may be gained from these resources. For example, cover crop biomass estimation via satellites (as described in Chapter 2) could provide a means of paying farmers based on the growth, or performance, of their cover crops. Performance-based cover crop payments could incentivize farmers to better manage cover crops, ultimately decreasing nutrients losses from fields and reducing potential contamination of ground and surface water. Plant growth regulators like trinexapac-ethyl have also existed for some time, but the effects on barley in the Mid-Atlantic region of the United States (discussed in Chapter 1) have not been previously reported in the literature. The main goal of plant growth regulators is to increase crop standability and maintain quality, which will become increasingly important as the need for greater production on the same amount of land increases.

Developing new technologies and becoming more precise in agriculture has been paramount in boosting crop yields and reducing fertilizer waste for decades and will continue to be important in the future. New satellite constellations like Planet are reducing the limitation of long revisit periods for satellite imagery and need to be compared to current free satellite imagery (as researched in Chapter 2). Novel techniques must also be investigated to improve upon practices that have remain relatively unchanged for decades. Soil sampling results for phosphorus fertilizer recommendations, for example, exhibit relatively high variability in terms of response to fertilizer application even when lab results imply a crop yield increase is likely. Current recommendations are based on lab methods, sample zone sizes, and yield response curves that may be able to be bested by new technology in the 21^{st} century. Chapter 3 investigated the use of an ‘indicator crop’ (i.e. a plant exhibiting a quantifiable response to variation in a soil property across an agricultural field), to delineate between areas of sufficient or deficient plant available phosphorus for subsequent cash crop growth. Not only could plant available phosphorus be more accurately determined via a living cover crop than a chemical laboratory analysis, but phosphorus availability mapped at finer spatial resolution than economically possible with traditional soil sampling.

Chapter 1: Trinexapac-Ethyl Rate and Timing Impact on Malt Barley Production in Virginia

ABSTRACT

Increased demand for locally-sourced inputs for breweries and distilleries creates an opportunity for Virginia farmers to grow barley (*Hordeum vulgare* L.) for malting, which can be sold for substantially more than feed barley. Lodging may decrease grain yield, reduce grain quality, and result in harvesting difficulties. Trinexapac-ethyl (TE) is a plant growth regulator designed to mitigate lodging risk by reducing cell elongation, creating a shorter and sturdier stem. Field studies were initiated in 2017 and 2018 to test TE effects on two barley cultivars (‘Flavia’ and ‘Violetta’) at two locations (Blackstone and Holland, VA). The study was designed as a randomized complete block with four replications at each site. Treatments consisted of: no TE applied; 62 g TE ha^{-1} and 125 g TE ha^{-1} applied at Zadoks growth stage (GS) 29; 62 g TE ha^{-1} and 125 g TE ha^{-1}applied at Zadoks GS32; and 125 g TE ha^{-1} equally split between GS29 and 32. Plant height, lodging incidence, and grain yield were measured for each plot. The effect of TE rate and timing varied between years and locations, but applications at GS32 always resulted in significantly decreased plant height. Plant lodging was decreased in 2019 at the Blackstone site by all TE applications compared to untreated. Plant height was decreased by as much as 42% in 2019 and plant injury was observed. Grain yield was decreased by all PGR applications in Blackstone and GS32 and split applications in Holland in 2019, presumably due to weather conditions preceding and following TE application. Plant growth at the time of application, observed and forecasted weather, and cultivar susceptibility to lodging should all be considered when determining the optimal TE

application rate and timing to reduce plant height without negatively impacting grain yield.

INTRODUCTION

Malting barley (*Hordeum vulgare* L.) is a critical ingredient for brewing beer and distilling whiskey and bourbon. The rising number of breweries and distilleries in Virginia combined with increasing demand for locally-grown ingredients in food and drinks is creating demand for Virginia-grown malting barley. This increased demand represents an opportunity for farmers to take advantage of grain prices considerably greater than barley grown for feed, which currently represents the majority of Virginia-grown barley. However, barley grown for feed is often managed with the goal of maximizing grain yield, whereas grain quality (e.g. kernel size and uniformity and grain protein concentration) affects desirability for malting (Henry, 1990; BMBRI, 2010; Singh, et al. 2014). Maltsters (i.e. purchasers of barley for malting) may reject grain if quality standards are not met.

Lodging, or the failure of small grains to remain standing upright (Pinthus, 1974), can decrease barley yield and quality by restricting the transport of nutrients from roots to the grain head, increasing grain left in the field due to harvestability issues, and increasing disease incidence (Day and Dickson, 1958; Singh, et al. 2014). Although lodging is often attributed to increased nitrogen application rates more typical of feed barley (Baethgen et al., 1995; O'Donovan, et al. 2011), barley grown for malting is still susceptible. Reducing plant lodging may help maintain grain quality and profitability for the farmer due to the increased importance of grain quality for malting (Baethgen et al., 1995; O'Donovan, et al. 2011).

The plant growth regulator (PGR) ethephon ([2-chloroethyl] phosponic acid) has been shown to decrease plant height (Bulman and Smith, 1993) and lodging (Thomason, et al., 2007) of small grains in the Mid-Atlantic US, but negative impacts on grain yield and test weight have been reported on a cultivar-dependent basis with ethephon application as well (Taylor et al., 1991; Thomason, et al. 2007). Trinexapac-ethyl (TE) {ethyl 4-[cyclopropyl(hydroxyl)methylene]-3,5-dioxocyclohexane-1-carboxylate} is a PGR that has been labeled for small grain application relatively recently in the US. Similar to ethephon, TE causes reduced stem elongation by inhibiting gibberellic acid production in the plant (Rademacher, 2000). However, TE sometimes elicits different physiological responses than other PGRs because gibberellic acid production is affected in a different part of the biosynthetic pathway of small grains (Hafner, 2001). Application of TE reduced malt barley (Miziniak et al., 2017) and lodging (Amabile et al. 2004) in Poland and Brazil without decreasing grain yield. Reduced plant height and lodging and increased grain yield have been observed in winter wheat in Michigan, US following TE application (Swoish and Steinke, 2017). However, the literature lacks data on TE applied to malting barley in the Mid-Atlantic region of the US. This study was designed to determine the effect of TE application rate and timing on two malting barley cultivars currently being commercially grown in Virginia, US.

MATERIALS AND METHODS

Research trials were established near Blackstone and Holland, VA, during the 2017/2018 and 2018/2019 growing seasons. Each location consisted of four replications of 12 plots measuring 4.9 m in length and 1.5 m in width arranged in a randomized complete block design. Plots were seeded at 538 seeds m^{-2} in 18-cm rows using a grain drill. Treatments consisted of either 0, 62, or 125 g TE ha^{-1} applied at growth stage (GS; Zadoks, 1974) 29 (leaf sheaths erect), 32 (second node visible), or split between GS29 and 32 (Table 1.1). The compound was surface-applied with a backpack sprayer at 93.5 liters ha^{-1} total output. The maximum labeled Palisade EC (Syngenta, Basel, Switzerland) rate for barley application (125 g TE ha^{-1}) will be referred to as the 'full' rate, whereas 'check' will refer to no TE application and 'half' to 62 g TE ha^{-1}. The product label recommends single applications to occur between GS29 and 32, and split applications in barley to occur first between GS29 and 31 and then again between GS32 and 37. First applications (i.e. GS29) occurred February 26th, 2018 and March 12th, 2019. Second applications (i.e. GS32) occurred April 20th, 2018 and April 7th, 2019. Each treatment was applied to cultivars 'Flavia' (Virginia Crop Improvement Association) and 'Violetta' (Limagrain Cereal Seeds, LLC), both of which are commonly used and easily attainable by Virginia farmers. Nitrogen fertilization rates and pest management practices for each individual location are detailed in Table 1.2. Average plant height per plot was measured at two places within each plot from the ground to tallest point at physiological maturity (Zadoks GS92). Lodging evaluations were made on a per-plot basis prior to harvest based on a zero-to-nine scale of visual lodging severity and incidence, with zero meaning no lodging and nine representing every plant in a plot lying flat on the ground (Szoke et al., 1979). Grain was harvested with a research plot combine equipped with a Graingage™ system (Juniper Systems, Logan, UT) for measuring grain yield per plot. Moisture and test weight were determined from a grain subsample from each plot using a DICKEY-john GAC2500 near infrared (NIR) grain analyzer (DICKEY-john, Auburn IL). Grain yield was corrected to 145 g water kg^{-1} for downstream calculations and comparisons.

Analysis of variance (ANOVA) was conducted using JMP Pro 14 (SAS Institute, 2018). Replication was treated as a random factor in each experiment and cultivar, application rate, and application timing were treated as fixed effects. When a significant F value was detected by ANOVA at $\alpha = 0.05$ treatment means were separated using Fisher's protected LSD.

RESULTS AND DISCUSSION

PGR Effect on Plant Height

Results were presented separately for 2018 and 2019 because plant height response to PGR was significantly different between study years. Cultivars were combined within locations because the interaction between location and treatment was significant for plant height in both years and the cultivar-treatment interaction was not. Similarly, Amabile et al. (2004) reported no interaction between cultivar and TE application on malting barley height across four varieties tested.

In 2018, untreated barley was 67 cm in Blackstone and 62 cm in Holland on average (Table 1.3). All TE applications significantly reduced plant height compared to the check. The GS29-Half treatment resulted in 7% shorter plants compared to untreated at both sites. No significant difference was observed by applying the full labeled rate of

TE (125 g ha^{-1}) compared to the half rate (64 g ha^{-1}) at GS29. Barley receiving a half rate at GS32 was significantly shorter than that receiving the half or full rate at GS29 in Blackstone, whereas in Holland GS32-Half resulted in shorter plants than GS29-Half but not GS29-Full. Full rates did not reduce height significantly more than half rates for either application timing at either site. Plants following split application in Blackstone were significantly taller than those treated with GS32-Full and not significantly different from plants receiving GS32-Half. Conversely, split application resulted in significantly shorter plants than all treatments except GS32-Full in Holland. The fact that split application did not result in shorter plants than GS32-Half in Blackstone, as was the case in Holland, indicates that successive applications do not always reduce plant height more than a single half-rate application at GS32. A significant difference was observed between GS29-Full and GS32 half in Blackstone only, meaning timing had a larger effect on plant height than rate in Blackstone compared to Holland. Variability in TE effect between locations may be due to differences in barley growth rate at the time of TE applications. Barley in Blackstone was treated with TE prior to spring N fertilizer applications, whereas TE application in Holland occurred following N fertilizer applications, possibly leading to increased barley growth rate.

Every PGR application in 2019 resulted in a greater observed reduction in plant height (Table 1.4) than the same application in 2018. In Blackstone the GS29-Half treatment significantly reduced plant height compared to no application, whereas in Holland it did not. The observed change in height between untreated and GS29-Half at Holland in 2019 (-8%) was greater than 2018 (-7%), indicating that lack of significance may have resulted from variability within replications and from analyzing only three replications instead of four. Other differences between sites in 2019 included shorter plants following split application compared to GS32-Half in Blackstone but not in Holland. Blackstone 2019 was only the only site-year in which GS32-Full and GS29-Full resulted in shorter plants than GS32-Half and GS29-Half, respectively.

Difference in plant height following PGR application in the literature did not exceed 16.5% in malting barley (Miziniak et al., 2016) and 27% in wheat (Rajala and Peltonen-Sainio, 2001; Matysiak, 2006; Swoish and Steinke, 2017), indicating that the extreme height decreases (i.e. > 30%) in Blackstone and Holland following GS32 and split treatments in 2019 were abnormal. These extreme height decreases were frequently accompanied by visual plant injury symptoms (e.g. chlorosis of leaves and stems) and decreased grain yield, which is discussed in further detail later in this paper. Injury to malting barley from TE application was not found elsewhere in the literature, but Wiersma et al. (2005) reported temporary chlorosis in wheat after TE application.

PGR Effects on Lodging

Plant lodging was minimal and not significantly different between treatments at either site in 2018 (data not shown). In 2019 lodging did not occur in Holland but was significantly reduced with PGR application at the Blackstone location (Table 1.5). Although lodging occurrence was statistically greater in the untreated plots, a rating of 1.1 (out of nine possible) represents only slight lodging that would not be expected to decrease grain yield or quality. Lodging presence was not severe enough to present harvestability issues, which is one of the other main concerns when lodging is extreme.

Effect of PGR on Grain Parameters

Grain parameters (i.e. yield, moisture, and test weight) differed between location and cultivar, but were not significantly different between treatments in 2018 for either location (Table 1.6). Similarly, Amabile et al. (2004) observed no difference in grain yield after TE application across four cultivars of irrigated malting barley in Brazil. Wheat (*Triticum aestivum* L.) grain yield has increased (Matysiak, 2006; Penckowski et al., 2009; Swoish and Steinke, 2017) or remain unchanged (Rajala and Peltonen-Sainio, 2002; Wiersma et al., 2011; Knott et al., 2016) following TE application in the majority of published studies. However, a negative effect on grain yield after PGR application occurred at both locations in the second year of this study for all but the GS29 applications in Holland (Table 1.7). Similarly, Espindula et al. (2009) found 125 g TE ha^{-1} decreased wheat yield, but 62 g TE ha^{-1} did not. The GS29-Half treatment reduced yield the least in Blackstone and was still 16% less than untreated barley. Grijalva-Contreras et al. (2012) observed grain yield decreases in wheat up to 13%, but only with greater TE rates than tested in this study (150 g TE ha^{-1}). Grain yield was significantly decreased by 41 – 42% in Holland following all treatments with TE application at GS32. Half and Full rates applied at GS29 in Holland also resulted in significantly greater grain moisture at harvest than untreated and GS29-Half treatments. Test weight in Holland was significantly less following GS32-Full compared to all treatments but GS29-Half.

The application of PGR after relatively cool air temperature and prior to relatively warm air temperature is believed to be the cause of plant injury in 2019 (Table 1.8). Gibberellic acid production in barley stems is highly dependent on growth temperature (Jusaitis et al., 1982). Plants in 2019 were likely treated with TE at periods of low gibberellic acid production, possibly causing exaggerated injury comparable to greater levels of TE application. The Palisade EC label cautions, "Do not apply if crop is stressed by drought, disease, or temperatures." Although unintentional, 2019 applications appear to have crossed the threshold of tolerable stress to barley in terms of temperature at both locations.

CONCLUSIONS

Trinexapac-ethyl successfully decreased the height of two barley cultivars by as much as 42%, exceeding observed reductions for other small grain crops in the literature. The half rate (64 g TE ha^{-1}) was as effective as the maximum labeled rate (125 g TE ha^{-1}) in three of four site-years for both the GS29 and GS32 application timings. Later applications (GS32) always decreased plant height more than GS29 applications for half and full rates. Split applications of 64 g TE ha^{-1} at GS29 and GS32 resulted in no further height decrease compared to 125 g TE ha^{-1} applied at GS32. All TE rate/timing combinations significantly reduced lodging compared to untreated in 2019 at the Blackstone site, though lodging severity was minimal. Substantial lodging did not occur at either site in either year, so conclusions on prevention of yield-limiting lodging in malting barley cannot be drawn from this study. TE did not affect grain yield in 2018, but all applications in 2019 except the GS29 timing in Holland resulted in significantly decreased grain yield compared to untreated barley.

Visible plant injury and subsequent yield reduction occurred when applications followed stressful weather conditions (i.e. cold and dry weather) and preceded periods favoring more rapid growth (i.e. increases in air temperature and adequate soil moisture). Applications of PGR to barley that has emerged from dormancy (i.e. green-up has visibly occurred) and is not expected to experience temperature or drought stress for approximately seven days may minimize risk of injury. A half-rate of TE applied relatively early in the season appears to be the safest and most economical option to reduce plant height and lodging. However, given the potential for plant injury, TE application to malting barley that is not prone to lodging may introduce unnecessary risk with limited potential for increased yield compared to untreated barley.

Table 1.1. Treatment details replicated four times in a randomized complete block design. GS = Growth stage, Zadoks scale.

Treatment	Cultivar	Rate	Application timing
		g TE ha^{-1}	
Check	Flavia	0	N/A
GS29-Half	Flavia	62	GS 29
GS29-Full	Flavia	125	GS 29
GS32-Half	Flavia	62	GS 32
GS32-Full	Flavia	125	GS 32
Split	Flavia	62 + 62†	GS 29 + 32
Check	Violetta	0	N/A
GS29-Half	Violetta	62	GS 29
GS29-Full	Violetta	125	GS 29
GS32-Half	Violetta	62	GS 32
GS32-Full	Violetta	125	GS 32
Split	Violetta	62 + 62	GS 29 + 32

†One application of 64 g trinexapac-ethyl ha^{-1} was applied at GS 29 and another at GS 32.

Table 1.2. Management practices and dates for each location and year.

Location	Harvest Year	Date	Action
Blackstone	2018	10/17/17	Nitrogen application (34 kg N ha^{-1})
		10/19/17	Planted into disked ground
		2/28/18	Nitrogen application (67 kg N ha^{-1})
		2/28/18	Herbicide application
		4/23/18	Nitrogen application (45 kg N ha^{-1})
		6/5/18	Harvested
	2019	10/19/18	Nitrogen application (34 kg N ha^{-1})
		10/24/18	Planted into disked ground
		2/6/19	Nitrogen application (67 kg N ha^{-1})
		2/6/19	Herbicide application
		3/27/19	Nitrogen application (67 kg N ha^{-1})
		3/27/19	Herbicide application
		6/3/19	Harvested
Holland	2018	10/17/17	Nitrogen application (39 kg N ha^{-1})
		10/25/17	Planted into disked ground
		2/5/18	Nitrogen application (67 kg N ha^{-1})
		3/21/18	Herbicide application
		4/3/18	Nitrogen application (56 kg N ha^{-1})
		4/3/18	Herbicide application
		4/26/18	Fungicide application
		6/6/18	Harvested
	2019	11/25/18	Nitrogen application (35 kg N ha^{-1})
		11/29/18	Planted into disked ground
		2/12/19	Nitrogen application (67 kg N ha^{-1})
		2/12/19	Herbicide application
		3/14/19	Nitrogen application (67 kg N ha^{-1})
		3/23/19	Herbicide application
		5/30/19	Harvested

Table 1.3. Effect of trinexapac-ethyl rate and timing on 'Flavia' and 'Violetta' barley growth in Virginia, USA, 2018. Height difference was assessed compared to untreated barley. Values followed by the same letter within location are not significantly different at α=0.05.

Location	Treatment	Plant Height		Height Difference
		cm		% change
Blackstone	Check	67	a	
	GS29-Half	63	b	-7
	GS29-Full	60	b	-10
	GS32-Half	52	cd	-22
	GS32-Full	49	d	-27
	Split	54	c	-20
Holland	Check	62	a	
	GS29-Half	57	b	-7
	GS29-Full	54	bc	-12
	GS32-Half	51	cd	-17
	GS32-Full	50	de	-19
	Split	48	e	-23

Table 1.4. Effect of trinexapac-ethyl rate and timing on 'Violetta' and 'Flavia' barley growth in Virginia, US, 2019. Height difference was assessed compared to untreated barley. Values followed by the same letter within location are not significantly different at α=0.05.

Location	Treatment	Plant Height		Height Difference
		cm		% change
Blackstone	Check	60	a	
	GS29-Half	49	b	-19
	GS29-Full	42	c	-30
	GS32-Half	42	c	-31
	GS32-Full	37	d	-39
	Split	36	d	-40
Holland	Check	61	a	
	GS29-Half	57	ab	-8
	GS29-Full	50	b	-19
	GS32-Half	36	c	-41
	GS32-Full	36	c	-42
	Split	36	c	-41

Table 1.5. Effect of trinexapac-ethyl rate and timing on 'Violetta' and 'Flavia' barley lodging severity (based on visual ratings of 0 – 9 on lodging severity in each plot) in Blackstone, Virginia, US, 2019. Values followed by the same letter within location are not significantly different at α=0.05.

Treatment	Lodging	
Check	1.1	a
Half Early	0.3	b
Full Early	0.1	b
Half Late	0.0	b
Full Late	0.0	b
Split	0.0	b

Table 1.6. Malt barley grain yield, moisture, and test weight in Virginia, US, 2018.

Location	Cultivar	Yield	Moisture	Test Weight
		Mg ha^{-1}	%	kg m^{-3}
Blackstone	Flavia	5.62	12.1	543
	Violetta	5.64	12.3	566
Holland	Flavia	5.28	13.3	563
	Violetta	4.92	13.4	580

Table 1.7. The effect of trinexapac-ethyl application rate and timing on 'Violetta' and 'Flavia' barley grain yield, moisture, and test weight in Virginia, US, 2019. Values followed by the same letter within location and column are not significantly different at α=0.05.

Location	Treatment	Yield		Moisture		Test Weight	
		Mg ha^{-1}		%		kg m^{-3}	
Blackstone	Check	3.22	a	13.4	a	566	a
	GS29-Half	2.67	b	13.6	a	553	a
	GS29-Full	2.70	b	13.6	a	572	a
	GS32-Half	2.28	bc	13.4	a	565	a
	GS32-Full	1.61	d	13.8	a	558	a
	Split	2.14	c	13.7	a	575	a
Holland	Check	3.27	a	11.8	b	611	a
	GS29-Half	2.95	a	11.9	b	611	a
	GS29-Full	2.65	a	12.2	ab	604	a
	GS32-Half	1.26	b	12.8	a	578	ab
	GS32-Full	1.42	b	13.0	a	526	b
	Split	1.40	b	12.3	ab	592	a

Table 1.8. Summary of weather data preceding and following trinexapac-ethyl application to barley for the 2018 and 2019 harvest seasons in Virginia, US.

			Average Daily Maximum Air Temperature (℃)		Precipitation (cm)	
Location	Application	Year	Week Preceding Application	Week Following Application	Week Preceding Application	Week Following Application
Blackstone	GS29	2018	19.4	13.3	0.66	1.65
		2019	8.9	17.8	0.53	0.00
	GS32	2018	24.4	19.4	3.30	4.65
		2019	17.2	23.3	1.32	1.70
Holland	GS29	2018	20.6	15.0	0.74	1.65
		2019	10.6	17.2	0.61	0.41
	GS32	2018	22.8	18.9	3.05	2.67
		2019	15.6	23.3	1.98	4.09

BIBLIOGRAPHY:

Alley, M. M., T. H. Pridgen, D. E. Brann, J. L. Hammons, and R. L. Mulford. 1997. Nitrogen fertilization of winter barley: principles and recommendations. Pub. No. 424-801, Virginia Coop. Ext., Blacksburg, VA.

Amabile, R. F., et al. 2004. "Efeito do regulador de crescimento Trinexapac-Etil em cevada cervejeira irrigada em áreas de Cerrado do Distrito Federal." Embrapa Cerrados-Boletim de Pesquisa e Desenvolvimento (INFOTECA-E).

Baethgen, W. E., Christianson, C. B. and Adrian, G. L. 1995. Nitrogen fertilizer effects on growth, grain yield, and yield components of malting barley. Field Crops Res 43: 87-99.

BMBRI. 2010. Quality factors in malting barley. Publ. 1510. A Brewing and Malting Barley Res. Inst., Winnipeg, MB, Canada.

Bulman, P., and D. L. Smith. 1993. Yield and grain protein response of spring barley to ethephon and triadimefon. Crop Sci. 33:798-803.

Day, A. D., and A. D. Dickson. 1958. "Effect of artificial lodging on grain and malt quality of fall-sown irrigated barley." Agronomy Journal (American Society of Agronomy) 50: 338-340.

Espindula, M.C., Rocha, V.S., Grossi, J.A.S., Souza, M.A., Souza, L.T. and Favorato, L.F. 2009. Use of growth retardants in wheat. Planta Daninha, 27, 379-387.

Grijalva-Contreras, R.L., Macías-Duarte, R., Martínez-Díaz, G., Robles-Contreras, F. and Nuñez-Ramírez, F. 2012. Effects of trinexapac-ethyl on different wheat varieties under desert conditions of Mexico. Agricultural Sciences, 3(05), p.658.

Hafner, V. 2001. Moddus—Universal product for lodging prevention in cereals. p. 167–172. In. Proc. Slovenian Conf. on Plant Protection, 5th. Catezob Savi, Slovenia. 6–8 March 2001.

Henry, R. J. 1990. Barley quality: an Australian perspective. Aspects of Applied Biology. 25, 5-14.

Jusaitis, M., Paleg, L.G. and Aspinall, D. 1982. The influence of gibberellic acid and temperature on the growth rate of *Avena sativa* stem segments. Plant physiology, 70(2), pp.532-539.

Knott, C. A., Van Sanford, D. A., Ritchey, E. L. & Swiggart, E. 2016. Wheat yield response and plant structure following increased nitrogen rates and plant growth regulator applications in Kentucky. Crop, Forage & Turfgrass Management, 2.

Matysiak, K. 2006. Influence of trinexapac-ethyl on growth and development of winter wheat. J. Plant Prot. Res. 46:133–143.

O'Donovan, J. T., T. K. Turkington, M. J. Edney, G. W. Clayton, R. H. McKenzie, P. E. Juskiw, G. P. Lafond, et al. 2011. Seeding rate, nitrogen rate, and cultivar effects on malting barley production. Agronomy Journal. 103: 709-716.

Penckowski, L. H., Zagonel, J. & Fernandes, E. C. 2009. Nitrogen and growth reducer in high yield wheat. Acta Scientiarum. Agronomy, 31, 473-479.

Pinthus, M.J. 1974. Lodging in wheat, barley, and oats: The phenomenon, its causes, and preventative measures. Advances in Agronomy. 25:209-263.

Rademacher, W. 2000. Growth retardants: effects on gibberellin biosynthesis and other metabolic pathways. Ann. Rev. Plant Biol. 51(1):501-531.

Rajala, A., and P. Peltonen-Sainio. 2001. Plant growth regulator effects on spring cereal root and shoot growth. Agronomy Journal. 93:936–943.

Rajala, A. & Peltonen-Sainio, P. 2002. Timing applications of growth regulators to alter spring cereal development at high latitudes. Agricultural and Food Science, 11, 233-244.

SAS Institute. 2012. The SAS system for Windows. Release 9.4. SAS Inst., Cary, NC.

Singh, Avtar, Harmeet Singh, J. S. Kang, and Jasvinder Singh. 2014. "Advancement Of Agronomic Practices In Malting Barley-A Review." International Journal of Current Research. 6 (02): 4921-4935.

Swoish, M., and K. Steinke. 2017. Plant growth regulator and nitrogen applications for improving wheat production in Michigan. Crop. Forage Turfgrass Manag. 3(1).

Szoke, T.G., J. Anthonissen, and J. Vergracht. 1979. New ethephon based anti-lodging product for barley. p. 843–852. In Proc. Int. Symp. on Crop Protectium, Ghent, Belgium. Faculteit Land-Bouwwetenschappen, Ghent, Belgium.

Taylor, J. S., K. R. Foster, and C. D. Caldwell. 1991. Ethephon effects on barley in central Alberta. Can. J. Plant Sci. 71:983-995.

Thomason, Wade E., Steve B. Phillips, Carl A. Griffey, and Wynse S. Brooks. 2007. "Hulless barley response to ethephon application." Crop Management. (Plant Management Network) 6: 0-0.

Wiersma, J. J., Beverly, R. and Camerum, J. N. 2005. Efficacy and crop safety of Trinexapac-ethyl to reduce plant height and improve straw strength in spring wheat. NCWSS Research Report.

Wiersma, J. J., Dai, J. & Durgan, B. R. 2011. Optimum timing and rate of trinexapac-ethyl to reduce lodging in spring wheat. Agronomy journal, 103, 864-870.

Zadoks, J. C., T. T. Chang, and D. F. Konzak. 1974. A decimal code for the growth stages of cereals. Weed. Res. 14:415-421.

Chapter 2: Comparing Satellites and Vegetation Indices for Cover Crop Biomass Estimation

ABSTRACT

Cost-share programs based on measures of participation rather than performance are available to farmers who plant cover crops. However, cover crops only provide significant ecological benefits like reduced nutrient loss when adequate biomass is established. The purpose of this study was to determine whether satellite imagery can effectively estimate cover crop biomass in fields with diverse species composition, and whether increased spatial resolution and satellite imaging frequency can increase biomass estimation accuracy. Aboveground biomass samples of $1m^2$ were collected for 86 sites within 26 agricultural fields containing unique cover crop species composition to assess biomass production. In-field sensors were used to measure normalized difference vegetation index (NDVI) and groundcover percentage. Three satellites (Landsat 8 [30 m resolution], Sentinel 2 [10 m resolution], and Planet [3 m resolution]) were used to calculate eight vegetation indices (VIs) for comparison with cover crop biomass. Multiple linear regression, correlation coefficients, and root mean square error (RMSE) were used to perform hierarchical clustering to rank VIs calculated from each satellite for biomass estimation accuracy. Satellites predicted cover crop biomass at the field level very accurately (up to 0.89 and 0.79 for correlation coefficient and r^2, respectively), demonstrating the potential of large-scale biomass estimation for relatively low cost compared to in-field sampling. All satellite-VI pairs more accurately estimated biomass than the in-field sensors. Performance of VIs varied by satellite, but each satellite had at least one VI that performed very well for both site-level and field-averaged data,

indicating that VI selection was more important than satellite selection. Despite frequent use in the literature, NDVI was not the best predictor of biomass for any satellite. Planet was the only satellite to provide useable imagery for every site due to increased revisit period; however, its increased spatial resolution did not increase estimation accuracy overall compared to Landsat 8 or Sentinel 2.

INTRODUCTION

A ‘cover crop’ is one or more plant species seeded between cash crops that is terminated either by cold temperatures or by the farmer, either chemically or mechanically. Cover crops can reduce nutrient losses to runoff and leaching (Jordan et al., 1994; Justes et al., 1999), increase soil organic matter percentage (Steenwerth and Belina, 2008), and reduce the need for chemical fertilization to the subsequent cash crop (Seo et al., 2006; Dean and Weil, 2009). Reduced nutrient loss can decrease eutrophication of surface water and pollution of groundwater- two major environmental concerns in regions of the United States with substantial agricultural production. In addition to environmental benefits, Weil and Kremen (2007) found that adding a cover crop into an agricultural system may improve farm profitability by reducing the need for fertilizer and pesticides. Grain yield increases averaging 2 – 3% in corn and soybean following cover crops have also been reported by surveyed farmers (Watts and Myers, 2016).

However, risks are associated with cover crop sowing as well. Most notably, the farmer is often subjected to all the financial risk even though benefits like reduced leaching and erosion are beneficial for the environment as a whole (Snapp et al., 2005).

Although cover crops have been used for centuries, the number of acres seeded to cover crops annually in the United States has more than doubled in the last decade (Watts and Myers, 2016). Presumably, the resurgence of this historic practice is either due to positive effects observed in-field by researchers and farmers and/or the development of cost-share payment programs by organizations such as the Natural Resources Conservation Service (NRCS).

A potential flaw in cost-share systems is encouraging participation for monetary gain without ensuring adequate cover crop performance to justify the expenditure. The likelihood of nutrient retention, erosion prevention, and most other inherent benefits of cover crops is positively correlated with biomass production (Seo et al., 2006; Dean and Weil, 2009; Hively et al., 2009). Therefore, a paradigm shift from participation-based cost share programs to a performance-based model may be warranted to further protect our water resources and promote better cover crop management. An accurate and relatively time- and cost-effective method of cover crop biomass estimation would help facilitate the enforcement of a performance-based model, as well expand the scope of cover crop monitoring beyond only those fields actively enrolled in cost share programs. By comparing growth over an entire watershed to nutrient loading and eutrophication of waterways we could more accurately evaluate the effects and perceived value of cover crops on agricultural fields.

Since manual collection of biomass samples for every field would be cost-prohibitive, satellite estimation of biomass has been proposed as early as 40 years ago (Tucker, 1980). Maas and Rajan (2008) used Landsat 8 (30 m resolution) satellite imagery to estimate ground cover of cash crops in Texas. Despite challenges associated with atmospheric interference and uncertainty of response, they found that satellite normalized difference vegetation index (NDVI) values were not significantly different than that from in-field NDVI values. In other words, biomass estimation was possible if clouds did not interfere with the imaging timeframe. Hively et al. (2009) demonstrated that biomass of grass monocultures was strongly correlated to NDVI values obtained from Landsat 8 in the Mid-Atlantic region of the United States ($r^2 = .81$). The literature lacks data on whether comparable results could be expected on mixtures of multiple cover crop species, which are gaining popularity in the United States (Smith et al., 2014; Anderson, 2016). Multi-species cover crop mixtures can sometimes result in greater benefits to soil physical, chemical, and/or biological properties than any single species can provide (Meisinger et al., 1991; Snapp et al., 2005). Different plant species reflect unique wavelengths of light, so NDVI-to-biomass correlations may not represent the wide range of cover crops that farmers sometimes plant. Other vegetation indices (VIs) should be evaluated to determine the effect of multi-species cover crop mixtures on biomass estimation.

Further research is also warranted to determine whether newer satellite imaging platforms offering pixel sizes as fine as 3 m (i.e. 100 times more data points in the same area as one 30 m pixel) may increase estimation accuracy. The 3 m imagery is captured daily in the Mid-Atlantic United States, compared to once every 3 – 16 days for most other satellites with near infrared (NIR) bands for NDVI calculation. Increased probability of cloud-free images due to increased imaging frequency and increased spatial resolution acknowledge two of the limitations previously cited for satellite remote sensing versus costly and destructive in-field sampling (Moran et al., 1997).

MATERIALS AND METHODS

Field sampling

A total of 86 cover crop samples were collected from 26 agricultural fields between 36.15 and 38.10° N latitude within the Ridge and Valley region of Virginia, US (Figure 2.1). The 86 sample locations (referred to hereafter as 'sites') were chosen within each field where cover crop growth appeared consistent for no less than 30 m in each direction. Three to four sites were sampled in each agricultural field. Each site was 50 m or more from the nearest field boundary or obstacle (e.g. trees within fields) to avoid non-target reflectance in satellite imagery. Fields that contained various combinations of grass (e.g. ryegrass, triticale), brassica (e.g. oilseed radish, turnip), and legume (e.g. hairy vetch, Austrian winter pea) species were chosen to assess whether accurate biomass estimations could be achieved across mixtures with heterogeneous plant architectures and leaf types (Table 2.1).

Sampling occurred in early to mid-December, prior to snow cover, and April, prior to termination, in 2016/2017 and 2017/2018. All aboveground vegetative biomass was collected from within a 1 m^2 template placed flat on the ground at each site. Cover crop species were separated and placed into labeled paper bags for subsequent processing. Three soil samples were collected from 0 – 30 cm depth in a 6 m diameter circle around each site. The application Canopeo® (Oklahoma State University, Stillwater, Oklahoma) was used to produce an estimate of green groundcover percentage by holding a Samsung Galaxy Note 5 (Samsung, Seoul, South Korea) camera adjacent to the site (to avoid photographing the template), perpendicular to the ground, and 1 m above the canopy. Handheld GreenSeeker® (Trimble Agriculture, Sunnyvale, California) and Crop Circle® (Holland Scientific, Lincoln, NE) sensors were used to record an average NDVI value for a 6 m-diameter circle around each site, 1 m above the canopy. The coordinates of each site were logged with a handheld GPSMAP® 62s GPS receiver (Garmin International, Inc., Olathe, Kansas) to subsequently locate pixels of interest during satellite imagery analysis.

Cover crop tissue and soil analysis

After field sampling, cover crop samples were oven-dried and weighed to determine dry biomass for each site. A subsample representing species composition on a percent dry matter basis was made for each site and ground to pass a 0.5 mm sieve. Total carbon and nitrogen (N) tissue percentage in subsamples was determined by an Elementar VARIO MAX® (Elementar, Langenselbold, Germany) combustion elemental analyzer. Aboveground biomass N uptake was calculated by multiplying the N tissue percentage of each site by the total biomass per hectare (weight of dry aboveground biomass for each site [kg m^{-2}] x 10,000). Soil samples were air-dried, ground to pass a 2 mm sieve, and analyzed for nitrate and ammonium concentration by potassium-chloride extraction using a Lachat Quickchem® 8500 flow injection autoanalyzer (Hach Company, Loveland, Colorado) with QuickChem sodium salicylate method 12-107-06-2-A (Hofer, 2001) and QuickChem 12-107-04-1-B using Cd reduction (Knepel, 2003), respectively. Analysis of variance (ANOVA) was conducted using JMP Pro 14 (SAS Institute, 2018). When a significant F value was detected by ANOVA at $\alpha = 0.05$ treatment means were separated using Fisher's protected LSD.

Satellite imagery analysis

Imagery from the date nearest to in-field sampling was downloaded from Landsat 8, Sentinel 2, and Planet satellites for all sites. If no imagery was available 21 days prior to or following in-field sampling then that site/satellite combination was considered a missing data point. Missing imagery was either due to cloud cover or field circumstances (e.g. snow cover or cover crop termination by the farmer) prohibiting acquisition. Vegetation index values were calculated for every site with each satellite's imagery using eight of the predefined 'Vegetation and Soils' indices in ArcGIS Pro 2.4.2 (Esri Inc., Redlands, California), summarized in Table 2.2. Field-derived GPS coordinates were imported to ArcGIS as points. Values of each VI were exported for statistical analysis for pixels corresponding to site coordinates.

JMP Pro 14 was used to perform linear regression analysis. Regressions were considered the best fit model for biomass based on VI values when correlation coefficient and r^2 was increased and root mean square error (RMSE) was decreased. Smaller RMSE corresponds to better biomass estimation accuracy since RMSE is an absolute measure of error (Hyndman and Koehler 2006). Relationships were tested for significance at α = 0.05.

Field-level data were also calculated for satellite VI values and biomass by averaging the 3 – 4 sites within each of the individual 26 agricultural fields sampled, creating a single VI and biomass average value per field. Field-level data were then analyzed with the same statistical methods as per-site data described above. Hierarchical cluster analysis (Ward method) was performed in JMP for site and field-average data for correlation coefficient, RMSE, and r^2 values of each satellite-VI pair. Site data resulted in three biomass estimation accuracy clusters (referred to as ‘good,’ ‘better,’ and ‘best’) and field-average data resulted in four clusters (referred to as ‘good,’ ‘better’, ‘much better’, and ‘best’). Cluster titles describe the comparative ability of satellite-VI pairs to estimate biomass as determined by similarity or dissimilarity of correlation, r^2, and RMSE to other satellite-VI pairs within this study.

RESULTS AND DISCUSSION

Cover crop and soil characteristics

Sites sampled had a similar or greater range of dry biomass production (Table 2.3) than other recent cover crop studies in the Mid-Atlantic region of the United States (Hively et al., 2009; Prabhakara et al., 2015; Finney et al., 2016; Curran et al., 2018). December biomass was predominately greater than 1000 kg ha^{-1}, which can significantly reduce nitrate loss compared to no cover crop (Hively et al., 2009). Groundcover also exceeded 60% for most sites; a rate that can reduce erosion by 80% (Daniel et al., 1999) and qualifies as “high residue cover” according to the Chesapeake Bay Program.

Cover crop tissue ranged from 1.79 – 6.23% N with a mean of 3.34%. Total aboveground biomass N uptake was significantly greater in sites without legumes compared to those with legumes for both fall and spring samples, likely due to greater biomass accumulation (Table 2.4). Fields without legumes were comprised primarily of grass species, which often produce the most biomass of any functional group. Neither soil nitrate nor ammonium concentrations were correlated with cover crop biomass, likely due to large observed variation in concentrations (data not shown). Because this study took place across a wide range of fields in western Virginia, the spatial variation of soil N within and among the agricultural fields sampled was likely too large for a strong relationship with cover cropping to be observed.

In-field Remote Sensing:

Only 27 Crop Circle values were available for analysis (of 86 possible) due to instrument failures in the field, but GreenSeeker and Crop Circle readings exhibited a strong correlation with one another for sites where both sensors were used (Figure 2.2). GreenSeeker resulted in greater correlation and r^2 and decreased RMSE for measured biomass compared to Crop Circle (Table 2.5), which could have been due to the number of available data points analyzed for each sensor or the specific samples compared. Values from each instrument plateaued as biomass increased (Figure 2.3A and B), similar to previous research with in-field sensors (Carlson and Ripley, 1997; Muñoz et al., 2010). Perry et al. (2012) observed an r^2 value of 0.30 between wheat or barley biomass and GreenSeeker readings, which was a weaker relationship than observed between GreenSeeker and polycultures in this study (r^2 =0 .47; Table 2.5). Species with different plant architecture exhibit different light reflectance properties (Muñoz et al., 2010), but the relationship between GreenSeeker values and dry aboveground biomass remained similar as the number of species increased (Table 2.6), indicating that the greater number of species did not negatively impact biomass estimation. Canopeo exhibited better potential to predict cover crop biomass than Crop Circle (i.e. greater correlation and r^2, decreased RMSE) and was similar to GreenSeeker (Table 2.5). Canopeo has the advantage of being free to anyone with a smartphone, making it the most easily accessible 'sensor.' However, groundcover values calculated by Canopeo are not a vegetation index, but rather simply a count of pixels in the green spectrum compared to those outside the green spectrum reported as a percentage. Groundcover percentage is useful for quantifying differences in plant vigor that are not easily observed by the naked eye but provides little valuable information after full groundcover is established because the returned value should always be near 100%, as observed in the abrupt plateau of Canopeo values in Figure 2.3C.

Satellite Remote Sensing

Values of VIs from 5 of the 86 total sites were determined to be outliers (i.e. more than two times the standard deviation of the expected value) and were not considered for statistical analysis of biomass estimation with satellite imagery. These outliers could have been due to unrepresentative field sampling or inaccuracy between in-field GPS coordinates and satellite pixels. Cloud-free imagery was only available for every sample site from Planet (Table 2.7), indicating that smaller revisit period (i.e. number of days between imaging for a specific location) was beneficial for estimating cover crop biomass in a timely matter. Landsat 8 had more site images available for analysis (n = 64) than Sentinel 2 (n = 53) despite a larger revisit period due to clouds coinciding with imaging dates. A significant positive relationship was observed between cover crop biomass and all VIs assessed, corroborating previous research on single VIs and/or cover crop monocultures (Tucker, 1979; Maas and Rajan, 2008; Hively et al., 2009; Frampton et al., 2013). Relationships were significant when data were separated for fall vs. spring samples as well, although relationships were much weaker due to the reduced number of observations and decreased biomass range. Relative accuracy of VIs were similar between fall and spring sampling, so satellite-VI pairs could be compared across sample timings. The RMSE, correlation, and r^2 values of each VI for cover crop biomass differed by satellite, presumably due to differences in radiometric quality, pixel size, and bandwidth (i.e. the range of a given band in nm). These statistical measures were combined for cluster analysis to determine which satellite-VI pairs were similar in terms of relationship to cover crop biomass (Figure 2.4).

Vegetation indices calculated from satellite imagery were a better predictor of cover crop biomass than in-field sensor values (Table 2.8; Table 2.5), although in-field sensors were not used over the same amount of area as the satellite pixels. In other words, satellite to in-field sensor comparisons are not based on the same area. Most notably, Landsat 8 represents much more area in one pixel than was sampled with Greeneeker, Crop Circle, or especially Canopeo, which could affect biomass estimation accuracy.

On a per-site basis, Planet PVI was the most accurate (RMSE = 470 kg biomass ha^{-1}, r^2 = .76; correlation coefficient = .87) estimator of cover crop biomass for all satellite-VI pairs analyzed and placing it in the 'best' accuracy cluster. Richardson and Wiegand (1977) used NIR band 6 (700 – 800 nm) and red band 5 (600 – 700 nm) of Landsat 2 when developing the original PVI formula. Similarities between Planet imagery and Landsat 2 imagery include NIR bandwidth (80 nm for Planet and 100 nm for Landsat 2), red bandwidth (80 nm for Planet and 100 nm for Landsat 2), and possibly radiometric quality lesser than Landsat 8 and Sentinel 2. These similarities may partially explain why PVI was the only VI calculated with Planet imagery to perform better than most VIs calculated with Landsat 8 or Sentinel 2 imagery despite greater spatial resolution. The most accurate Landsat 8 VI was PVI as well (RMSE = 495 kg biomass ha^{-1}; r^2 = .72; correlation coefficient = .85), also grouping within the 'best' accuracy cluster. Conversely, PVI was the only Sentinel VI to be ranked as 'good' accuracy as opposed to 'better' or 'best'. Sentinel 2 band 8's relatively large NIR bandwidth (767 – 908) and small red bandwidth (646 – 685) may not be conducive to biomass estimation with the PVI formula. Sentinel 2 NIR band 8a (848 – 881 nm) more closely matches the bandwidth of the other two satellites in this study, but the 20 m pixel size is inconsistent with the 10 m visible-spectrum bands.

Sentinel 2 RVI was the third (of three) VI in the 'best' accuracy cluster, dissimilar to Planet and Landsat 8. Sentinel may have performed best with RVI because RVI was developed using Landsat 1 NIR band 7, which had a bandwidth (800 to 1,100 nm) more similar to Sentinel 2 band 8 than either of the other satellite's NIR band in this study. Normalized difference vegetation index is much more widely used in the literature with Landsat 8 and Sentinel 2 for biomass studies (Tucker et al., 1985; Maas and Rajan; 2008; Hively et al., 2009; Frampton et al., 2013; Sibanda et al., 2015), but it was either 'better' (Landsat 8, Sentinel 2) or 'good' accuracy (Planet) for the satellites in this study compared to other VIs. Vaiopoulos et al. (2004) determined NDVI provided more accurate estimation of vegetation cover than RVI when analyzing Landsat 7 imagery, but that differences may be minor depending on soil reflectance. Since NDVI was developed as a modified form of RVI intended to reduce soil background noise (Rouse et al., 1974) it is not surprising that RVI performed similarly-to or better-than NDVI given the relatively dense vegetation in this study.

Although indices using green light reflectance are less common in the literature, CIG and GNDVI performed relatively well for both Landsat 8 and Sentinel 2 (‘better’ accuracy for both satellites). Similarly, Hunt Jr. et al. (2013) found CIG and GNDVI to outperform RVI, NDVI, SAVI, and MSAVI2 when analyzing Landsat 5 Thematic Mapper imagery. Landsat 8 results in the present study were better with CIG and GNDVI (‘better’ accuracy) compared to SAVI and MSAVI (‘good’ accuracy) as well. Green light reflectance may be more uniform across multiple cover crop species than red light absorption, which could explain the effectiveness of VIs using green light in this study compared to more commonly used VIs such as NDVI. Another possible reason for increased accuracy with VIs using green light may be lack of red-light interference in low biomass areas due to soil light interference.

The soil-adjusted VIs (i.e. MSAVI2, SAVI, and TSAVI all ranked as ‘good’ accuracy for Planet and ‘better’ for Sentinel 2. For Landsat 8 TSAVI was in the ‘better’ cluster and SAVI and MSAVI2 were in the ‘good’ cluster. Inconsistent and relatively poor results overall for these three indices compared to others tested may be partially attributable to the methods used in this study, in which the vegetation cover adjustment factor for SAVI and soil adjustment factor for TSAVI (Table 2.2) were held constant for comparison. The default values of ArcGIS were used for consistency across all sites. The soil correction values that the user is required to input should be based on the amount of vegetative cover in the area of interest, which was what this study is trying to identify with satellite imagery. Furthermore, soil-adjusted indices may not have been ideal for this study due to predominantly high groundcover, decreasing the need for soil correction (Xue and Su, 2017).

Field-Average Data:

When site data were averaged within each field, RMSE values decreased and correlation coefficients increased overall (Figure 2.5), indicating a greater degree of biomass estimation accuracy. Landsat 8 resulted in smaller RMSE values than Sentinel 2 and Planet for every VI. Hierarchical clustering revealed four accuracy clusters for field-average data (Figure 2.5), with 'much better' being added to the accuracy cluster descriptions between 'better' and 'best'. With five of eight of the 'best' accuracy VIs, Landsat 8 was most effective at estimating biomass at field-scale if choosing a VI at random. The relatively large pixel size of Landsat 8 may estimate biomass very well at field-scale due to collecting reflectance over more area per pixel. Furthermore, the relatively large tile size (i.e. the extent of each individual satellite image) of Landsat 8 resulted in more fields being compared *within* tiles as opposed to *across* several tiles. This may provide an advantage by minimizing variation in weather, angle of incidence, and other sources of potential error between smaller satellite tiles. The 16-day revisit period was not detrimental to the Landsat 8 estimation efficacy, but it did result in 3 fields with no imagery available. Planet PVI was the only Planet VI that ranked in the 'best' cluster, indicating that the main advantage of Planet data at the field-average level is increased revisit period.

CONCLUSIONS

For the purposes of large-scale cover crop biomass estimation, Landsat 8 proved highly capable with site- and field-level data if cloud-free imagery was available. Sentinel 2 did not perform as well as Landsat 8 despite increased revisit period and spatial resolution but could potentially be used in tandem with Landsat 8 to increase temporal resolution of free imagery. Planet's superior revisit period increases the amount of cloud-free imagery within a short temporal window and would be the most viable of the three satellites tested for detecting temporal changes of plant biomass in areas with frequent cloud cover. Planet's smaller pixel size (3 m) is useful for visualizing field boundaries and structures, which can be difficult with Sentinel 2 (10 m) and Landsat 8 (30 m). However, larger pixel size tended to better estimate biomass across most VIs.

Each satellite had one of the three 'best' accuracy VIs for site data, indicating that VI selection affected predictive accuracy more than from which satellite imagery was sourced. Despite the widespread use of NDVI in the literature, other VIs were more accurate for cover crop biomass estimation in all three satellite imagery sources. When using Planet or Landsat 8 imagery, PVI should be used for cover crop biomass estimation on a per-site basis and RVI should be used when using Sentinel 2 imagery. Field-average data increased estimation accuracy overall and resulted in eight VIs in the 'best' accuracy cluster, suggesting that for large-scale biomass estimation, averaging multiple points within agricultural fields would be beneficial. Multiple cover crop species at each site did not prevent the expected positive relationship between VI values and aboveground biomass, but further research should explore the effect of plant architecture in multi-species mixtures on reflectance and VIs. This study suggests much potential for satellite remote sensing in agriculture, and collection of more biomass to compare across a wider range of satellite data and VIs could very likely increase estimation accuracy and confidence intervals further. Satellite remote sensing is therefore a strong candidate for performance-based cover crop payments in Virginia.

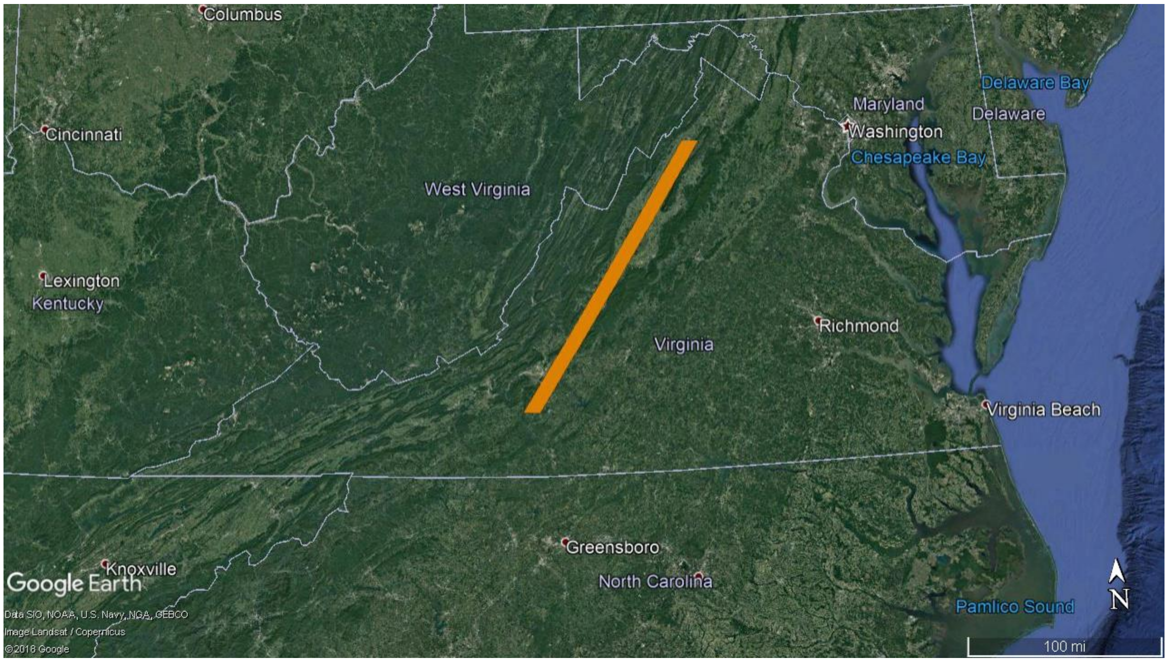

Figure 2.1. An orange line representing the approximate geographic range the agricultural fields in this study were located.

Table 2.1. Cover crop mix characteristics across 86 sites in Virginia, USA. Grasses, legumes, and brassicas were present in 82, 50, and 20 sites, respectively.

Parameter	Minimum	Maximum	Mean	Standard Deviation
Species (number site^{-1})	2	6	3	1
Grass biomass (percent of total biomass site^{-1})	0	100	72	31
Legume biomass (percent of total biomass site^{-1})	0	100	23	31
Brassica biomass (percent of total biomass site^{-1})	0	51	5	13

Table 2.2. Description of vegetation indices. NIR = pixel values from the near-infrared band; Green = pixel values from the green band; Red = pixel values from the red band; a = slope of the soil line (0.3 used for this study); b = gradient of the soil line (0.5 used for this study); L = amount of green vegetation cover (0.5 used in this study); s = the soil intercept line (0.5 used for this study); X = an adjustment factor to minimize soil noise (1.5 used for this study).

Index	Acronym	Formula	Source
Chlorophyll index- green	CIG	$\frac{NIR}{Green - 1}$	Gitelson et al., 2003
Green normalized difference vegetation index	GNDVI	$\frac{NIR - Green}{NIR + Green}$	Gitelson et al., 1996
Modified soil adjusted vegetation index	MSAVI2	$0.5 * (2(NIR + 1) - \sqrt{(2 * NIR + 1)^2 - 8(NIR - Red)})$)	Qi, J. et al., 1994
Normalized difference vegetation index	NDVI	$\frac{NIR - Red}{NIR + Red}$	Rouse Jr. et al., 1974
Perpendicular vegetation index	PVI	$\frac{(NIR - a * Red - b)}{(\sqrt{1 + a^2})}$	Bannari et al., 1996
Soil adjusted vegetation index	SAVI	$\frac{NIR - Red}{NIR + Red + L} * (1 + L)$	Huete, A. R., 1988
Ratio vegetation index	RVI	$\frac{NIR}{Red}$	Birth and McVey, 1968
Transformed soil adjusted vegetation index	TSAVI	$\frac{a * (NIR - a * Red - s)}{s * NIR + Red - s * a + X * (1 + a^2)}$	Baret, F. and Guyot, G., 1991

Table 2.3. Physical properties of sampled cover crop biomass from 86 sites in Virginia, USA.

	Dry Biomass kg ha^{-1}	Groundcover %
	Fall	
Minimum	571	37
Maximum	3258	98
Mean	1738	81
Standard Deviation	615	14
	Spring	
Minimum	1129	40
Maximum	5954	100
Mean	3261	92
Standard Deviation	1031	10

Table 2.4. Comparison of sites with and without legume cover crops present. Values followed by the same letter within sample timings are not significantly different at α=0.05.

Sample Timing		Aboveground Biomass N Uptake	
		kg ha^{-1}	
Fall	With Legumes	46	b
	Without Legumes	78	a
Spring	With Legumes	85	b
	Without Legumes	114	a

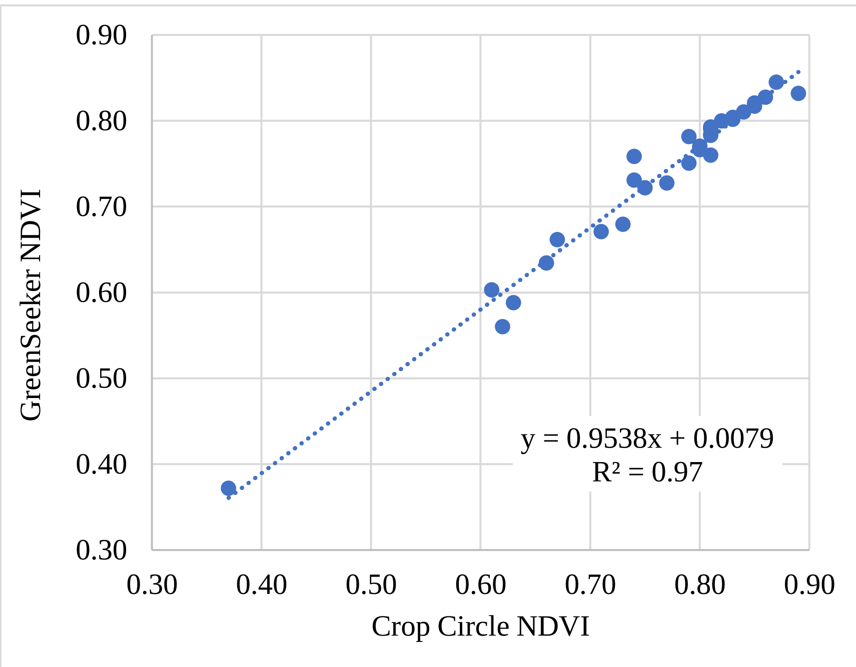

Figure 2.2. The relationship between GreenSeeker and Crop Circle readings from 27 sites of mixed cover crop stands in Virginia, US.

Table 2.5. Comparison of the relationship between in-field remote sensor values and mixed-species cover crop biomass across 86 sites in Virginia, US. Correlation is between sensor values and dry aboveground cover crop biomass. P values are at α = 0.05.

Sensor	Correlation	P-value	r^2	RMSE	Sample Size
				kg ha^{-1}	n
Canopeo	0.63	<.0001	0.51	733	86
Crop Circle	0.57	0.0018	0.33	915	27
GreenSeeker	0.68	<.0001	0.47	762	86

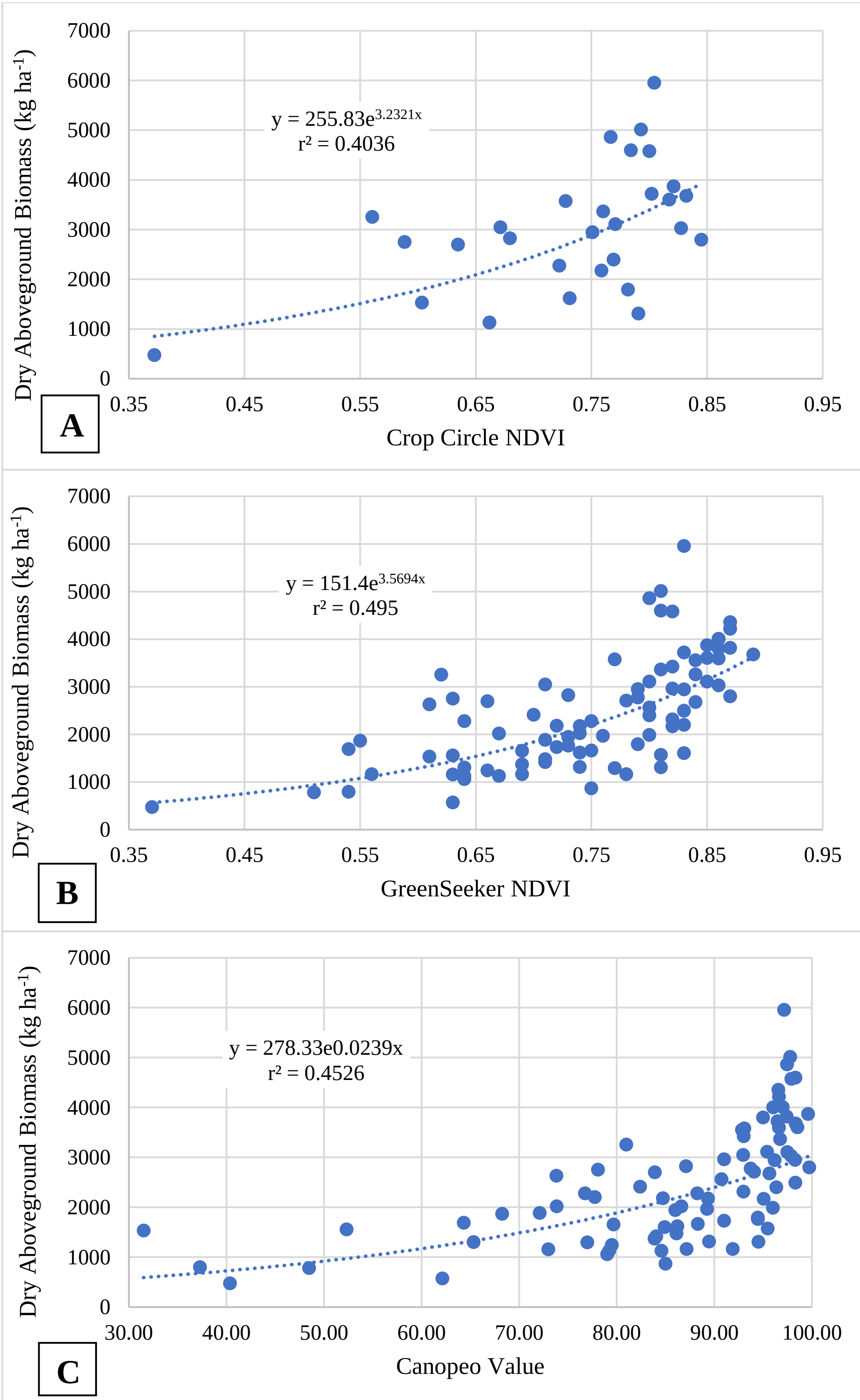

Figure 2.3. The relationship between cover crop biomass and Crop Circle (A), GreenSeeker (B), and Canopeo (C) values. Logarithmic trendlines represent sensor values plateauing at increased biomass.

Table 2.6. Comparison of the relationship between GreenSeeker values and mixed-species cover crop biomass averaged for 3 – 4 sites within 26 agricultural fields at increasing species diversity in Virginia, USA. Data for greater than four species per field were combined due to small sample size for individual species quantities. Correlation is between GreenSeeker values and dry aboveground cover crop biomass. P values are at α = 0.05.

Number of Species	Correlation	P-value	r^2	Sample Size
2	0.72	0.013	0.51	11
3	0.75	0.021	0.56	9
4+	0.75	0.012	0.57	10

Table 2.7. Characteristics of satellites used for determination of vegetation index values. Imagery available refers to number of cloud free images available within 21 days of field sampling (of 81 maximum). Revisit period refers to the approximate minimum number of days between images in Virginia, USA. Only Sentinel-2A data was available for year 1 of this study, resulting in a 10 day revisit period. Sentinel 2 A and B now result in a 5-day revisit period.

Satellite	Sites with Imagery Available	Pixel size	Revisit Period	Green Band (wavelength range in nm)	Red Band (wavelength range in nm)	NIR Band (wavelength range in nm)
Landsat 8	64	$30m^2$	16	Band 3 (530-590)	Band 4 (640-670)	Band 5 (850-880)
Sentinel 2	53	$10m^2$	5	Band 3 (537-582)	Band 4 (646-685)	Band 8 (767-908)
Planet	81	$3m^2$	1	Band 2 (500-590)	Band 3 (590-670)	Band 4 (780-860)

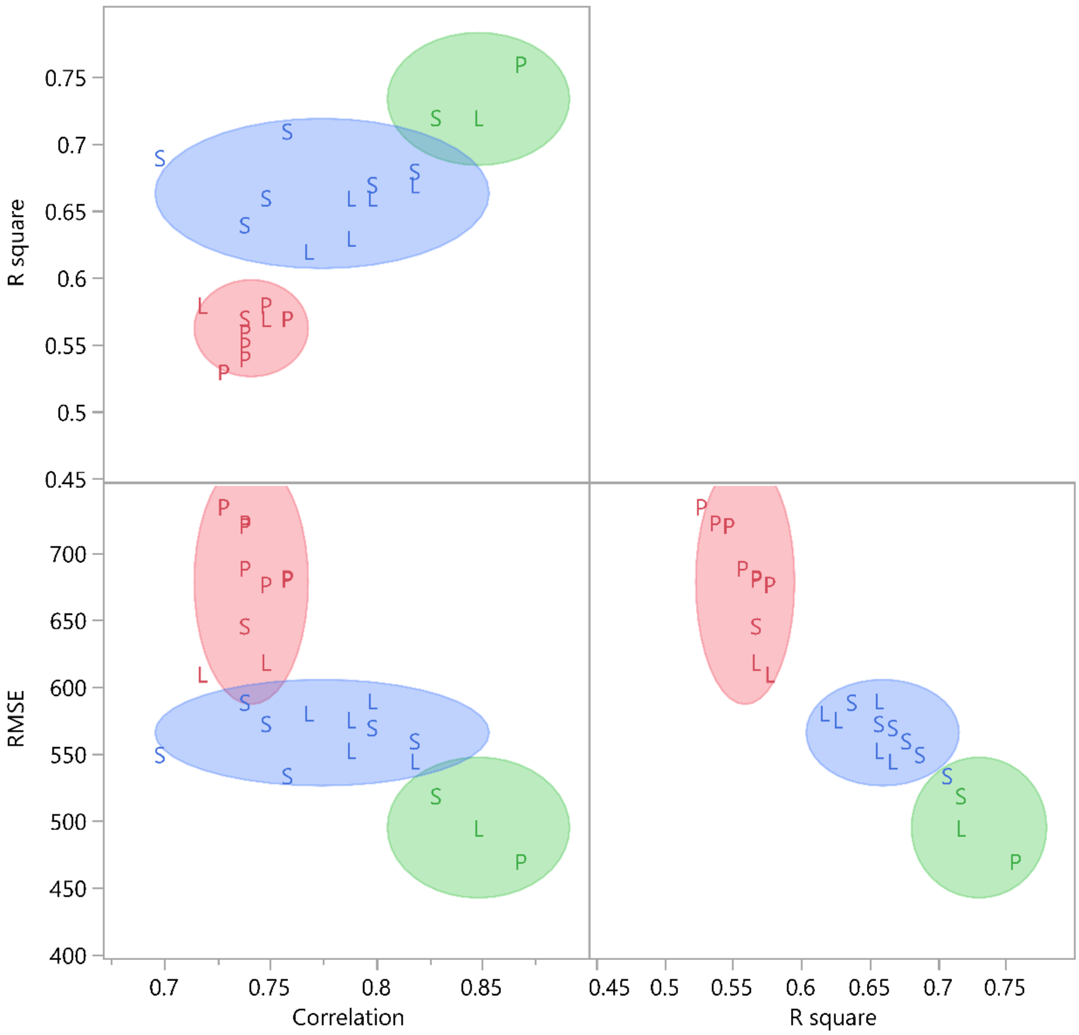

Figure 2.4. Hierarchical clustering of the correlation coefficient, r^2, and RMSE values of each satellite-VI pair compared to cover crop biomass for each site. Cluster 1 (green letters and ellipse) represents the 'best' accuracy for biomass prediction compared to other satellite-VI pairs, cluster 2 (blue letters and ellipse) represents 'better' accuracy, and cluster 3 (red letters and ellipse) represents 'good' accuracy. RMSE units are kg dry aboveground biomass ha^{-1}. "P" represents the satellite Planet, "L" represents Landsat 8, and "S" represents Sentinel 2.

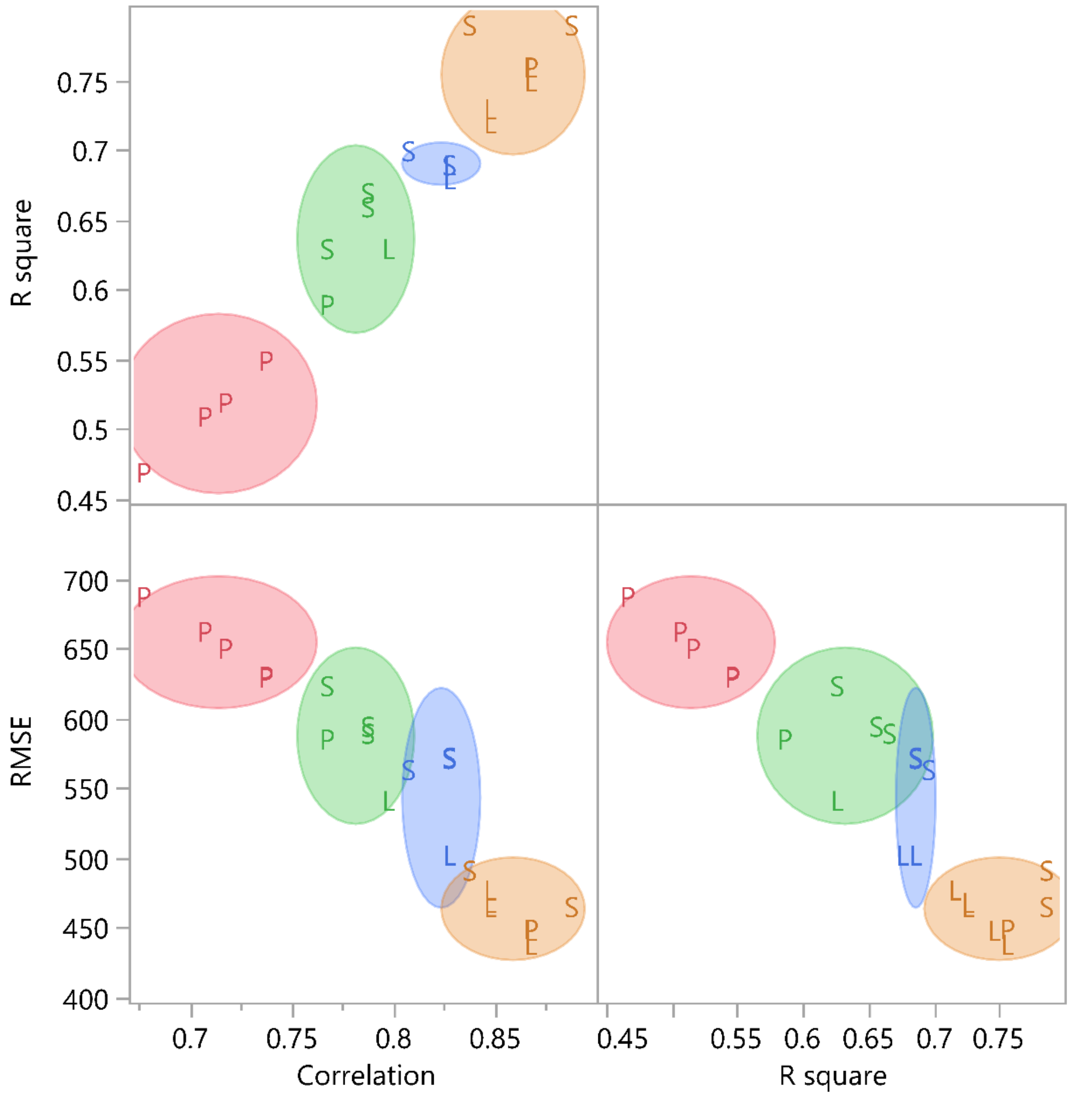

Figure 2.5. Hierarchical clustering of the correlation coefficient, r^2, and RMSE values of each satellite-VI pair compared to cover crop biomass average across 3 – 4 sites per agricultural field. Cluster 1 (orange letters and ellipse) represents the 'best' accuracy for biomass prediction compared to other satellite-VI pairs, cluster 2 (blue letters and ellipse) represents 'much better' accuracy, cluster 3 (green letters and ellipse) represents 'better' accuracy, and cluster 4 (red letters and ellipse) represents 'good' accuracy. RMSE units are kg dry aboveground biomass ha^{-1}. "P" represents the satellite Planet, "L" represents Landsat 8, and "S" represents Sentinel 2.

BIBLIOGRAPHY

Anderson, R.L. 2016. Considering canopy architecture when planning cover crop mixtures. Renewable Agriculture and Food Systems, 1–3.

Bannari, A., Huete, A.R., Morin, D. and Zagolski, F. 1996. Effects of soil color and brightness on vegetation indexes. International Journal of Remote Sensing, 17(10), pp.1885-1906.

Baraibar, B., Mortensen, D.A., Hunter, M.C., Barbercheck, M.E., Kaye, J.P., Finney, D.M., Curran, W.S., Bunchek, J. and White, C.M. 2018. Growing degree days and cover crop type explain weed biomass in winter cover crops. Agronomy for sustainable development, 38(6), p.65.

Baret, F. and Guyot, G. 1991. Potentials and limits of vegetation indices for LAI and APAR assessment. Remote sensing of environment, 35(2-3), pp.161-173.

Birth, G.S. and McVey, G.R. 1968. Measuring the color of growing turf with a reflectance spectrophotometer 1. Agronomy Journal, 60(6), pp.640-643.

Carlson, T. N. & Ripley, D. A. 1997. On the relation between NDVI, fractional vegetation cover, and leaf area index. Remote sensing of Environment, 62, 241-252.

Daniel, J.B., Abaye, A.O., Alley, M.M., Adcock, C.W. and Maitland, J.C. 1999. Winter annual cover crops in a Virginia no-till cotton production system: II. Cover crop and tillage effects on soil moisture, cotton yield, and cotton quality. J. Cotton Sci, 3(3), pp.84-91.

Dean, J.E. and Weil, R. 2009. Brassica cover-crops for N retention in the Mid-Atlantic Coastal Plain. J. of Environmental Quality, 38:520–528.

Finney, D.M., White, C.M. and Kaye, J.P. 2016. Biomass production and carbon/nitrogen ratio influence ecosystem services from cover crop mixtures. Agronomy Journal, 108(1), pp.39-52.

Frampton, W. J., Dash, J., Watmough, G. & Milton, E. J. 2013. Evaluating the capabilities of Sentinel-2 for quantitative estimation of biophysical variables in vegetation. ISPRS journal of photogrammetry and remote sensing, 82**,** 83-92.

Gitelson, A.A., Kaufman, Y.J. and Merzlyak, M.N. 1996. Use of a green channel in remote sensing of global vegetation from EOS-MODIS. Remote sensing of Environment, 58(3), pp.289-298.

Gitelson, A.A., Viña, A., Arkebauer, T.J., Rundquist, D.C., Keydan, G. and Leavitt, B. 2003. Remote estimation of leaf area index and green leaf biomass in maize canopies. Geophysical Research Letters, 30(5).

Hively, W. D., Lang, M., Mccarty, G. W., Keppler, J., Sadeghi, A. & MCCONNELL, L. L. 2009. Using satellite remote sensing to estimate winter cover crop nutrient uptake efficiency. Journal of soil and water conservation, 64**,** 303-313.

Hofer, S. 2001. QuikChem Method 12-107-06-2-A: Determination of ammonia (salicylate) in 2

M KCl soil extracts by flow injection analysis. Lachat Instrum., Milwaukee, WI.

Huete, A.R. 1988. A soil-adjusted vegetation index (SAVI). Remote sensing of environment, 25(3), pp.295-309.

Hunt Jr, E.R., Doraiswamy, P.C., McMurtrey, J.E., Daughtry, C.S., Perry, E.M. and Akhmedov, B. 2013. A visible band index for remote sensing leaf chlorophyll content at the canopy scale. International Journal of Applied Earth Observation and Geoinformation, 21, pp.103-112.

Hyndman, R. J. & Koehler, A. B. 2006. Another look at measures of forecast accuracy. International journal of forecasting, 22**,** 679-688.

Jordan, J.L., Morgan, S.L., and Elnagheeb, A.H. 1994. An Economic Analysis of Cover Crop Use in Georgia to Protect Groundwater Quality. Research Bulletin #419. Univ. of Georgia, College of Agric. and Environ. Sciences, Athens, Ga. 13.

Justes, E., Mary, B., and Nicolardot, B. 1999. Comparing the effectiveness of radish cover crop, oilseed rape volunteers and oilseed rape residues incorporation for reducing nitrate leaching. Nutrient Cycling in Agroecosystems, 55(3):207–220.

Knepel, K. 2003. QuikChem Method 12-107-04-1-B: Determination of nitrate in 2M KCl soil extracts by flow injection analysis. Lachat Instrum., Milwaukee, WI.

Maas, S. J. & Rajan, N. 2008. Estimating ground cover of field crops using medium-resolution multispectral satellite imagery. Agronomy Journal, 100**,** 320-327.

Meisinger, J.J., Hargrove, W.L., Mikkelsen, R.L., Williams, J.R. and Benson, V.W. 1991. Effects of cover crops on groundwater quality. Cover crops for clean water, pp.57-68.

Miziniak, W., Matysiak, K. & Kaczmarek, S. 2016. Studies on trinexapac-ethyl dose reduction by combined application with adjuvants in spring barley. Journal of Plant Protection Research, 57**,** 36-42.

Moran, M.S., Inoue, Y., and Barnes, E.M. 1997. Opportunities and limitations for image-based remote sensing in precision crop management. Remote Sensing of Environment, 61(3):319–346.

Muñoz, J. D., Finley, A. O., Gehl, R. & Kravchenko, S. 2010. Nonlinear hierarchical models for predicting cover crop biomass using Normalized Difference Vegetation Index. Remote Sensing of Environment, 114, 2833-2840.

Perry, E., Fitzgerald, G., Poole, N., Craig, S. & Whitlock, A. 2012. NDVI from active optical sensors as a measure of canopy cover and biomass. International Archives of the Photogrammetry, Remote Sensing and Spatial Information Sciences, 39, B8.

Prabhakara, K., Hively, W.D. and McCarty, G.W. 2015. Evaluating the relationship between biomass, percent groundcover and remote sensing indices across six winter cover crop fields in Maryland, United States. International Journal of Applied Earth Observation and Geoinformation, 39, pp.88-102.

Qi, J., Chehbouni, A., Huete, A.R., Kerr, Y.H. and Sorooshian, S. 1994. A modified soil adjusted vegetation index. Remote sensing of environment, 48(2), pp.119-126.

Rouse Jr, J., Haas, R.H., Schell, J.A. and Deering, D.W., 1974. Monitoring vegetation systems in the Great Plains with ERTS.

Seo, J.H., Meisinger, J.J., and Lee, H.J. 2006. Recovery of Nitrogen-15-labeled hairy vetch and fertilizer applied to corn. Agron. J., 98:245-254.

Sibanda, M., Mutanga, O. & Rouget, M. 2015. Examining the potential of Sentinel-2 MSI spectral resolution in quantifying above ground biomass across different fertilizer treatments. ISPRS Journal of Photogrammetry and Remote Sensing, 110**,** 55-65.

Smith, R.G., Atwood, L.W., and Warren, N.D. 2014. Increased Productivity of a Cover Crop Mixture Is Not Associated with Enhanced Agroecosystem Services. PloS one, 9(5),e97351.

Snapp, S., Swinton, S., Labarta, R., Mutch, D., Black, J., Leep, R., Nyiraneza, J. & O'Neil, K. 2005. Evaluating cover crops for benefits, costs and performance within cropping system niches. Agronomy journal, 97**,** 322-332.

Steenwerth, K. and Belina, K.M. 2008. Cover crops enhance soil organic matter, carbon dynamics and microbiological function in a vineyard agroecosystem, Applied Soil Ecology, 40(2):359–369.

Tucker, C. J. 1979. Red and photographic infrared linear combinations for monitoring vegetation. Remote sensing of Environment, 8**,** 127-150.

Tucker, C.J. 1980. A critical review of remote sensing and other methods for non-destructive estimation of standing crop biomass. Grass and Forage Science, 35(3), pp.177-182.

Tucker, C. J., Vanpraet, C. L., Sharman, M. J. & Van Ittersum, G. 1985. Satellite remote sensing of total herbaceous biomass production in the Senegalese Sahel: 1980--1984. Remote sensing of environment, 17**,** 233-249.

Watts, C. and Myers, R. 2016. Annual Report. 2015-2016 Cover Crop Survey. Sustainable Agriculture Research and Education/Conservation Technology Information Center, College Park, MD.

Weil, R. and Kremen, A. 2007. Thinking across and beyond disciplines to make cover crops pay. J. Sci. Food Agric. 87:551–5

Xue, J. and Su, B. 2017. Significant remote sensing vegetation indices: A review of developments and applications. Journal of Sensors, 2017.57.

Chapter 3: Evaluating the Use of an 'Indicator Crop' for Estimation of Plant Available Soil Phosphorus with Remote Sensing

ABSTRACT

Soil samples representing large land areas (i.e., 1 – 5 hectares) may incorrectly estimate phosphorus (P) fertilizer needs for optimal agronomic crop production, increasing potential for economic loss by under-fertilizing or P loss to ground and surface water by over-fertilizing. *Arabidopsis thaliana* Inositol Phosphate Kinase 1 loss-of-function mutant (*ipk1*$^-$), an inorganic phosphate-sensitive mutant of wild-type *Arabidopsis thaliana*, was used to assess the relationship between P concentration of growth media and plant growth. The overall goal was to determine the feasibility of using remote sensing in conjunction with an 'indicator crop' to map plant available P at greater spatial resolution than economically possible with traditional soil sampling. Three replications of 2, 4, and 6 *ipk1*$^-$ mutants per pot were grown in growth chambers across 9 P rates (0, 5, 10, 15, 25, 30, 40, 50, and 60 mg kg^{-1} P) arranged as a factorial design in vermiculite growth media with a continuous supply of macro- and micronutrient solution with no added P. Growth was assessed by measuring fractional green canopy cover (FGCC) and aboveground plant biomass one month after seeding. Dry biomass per plant and FGCC per plant were highly correlated (r^2 = 0.94). A significant quadratic relationship between FGCC and media P concentration at 2, 4, and 6 plants per pot (R^2 = 0.56, 0.79, and 0.89, respectively) was observed. The quadratic relationship's maximum occurred within the range of P fertilization decision making for maize grown in Virginia (i.e. 0 – 55 mg kg^{-1} P), resulting in difficulty differentiating between P concentrations

requiring or not requiring fertilizer without some previous knowledge of soil P range. The measurable relationship between plant FGCC and media P concentration validates the ability of an indicator crop to predict plant available nutrient levels and should be further explored.

INTRODUCTION

Phosphorus (P) is one of the most commonly applied nutrients to support crop growth in Virginia, US. The application of P to an agricultural field may be in response to soil testing and subsequent P fertilizer recommendations, or as manure applied primarily for other fertility goals. Leaching of P can increase markedly when P-containing fertilizers are added to soil already sufficient for crop production (Preedy et al., 2001; Bermudez and Mallarino 2007). Eutrophication (i.e. excessive nutrient buildup in water bodies which can result in catalyzed plant growth and subsequent dead zones) can occur when excess P in runoff enters a body of water (Carpenter, 2008; Todd et al., 2010; Tiessen et al., 2011). Loss of P from agricultural fields can also alter the species composition of wetland ecosystems (Grunwald et al., 2004). The amount of P lost to the environment, as well as economic loss for the farmer, can be reduced with proper rates and precise placement of fertilizer.

Several factors make precise P management difficult or economically impractical in production agriculture. Current phosphorus fertilizer recommendations rely on soil sampling and testing methods that contain potential sources of human error (e.g. soil cores must be pulled consistently and properly in the field). Soil samples for nutrient management often represent areas of 1 – 5 hectares, using approximately one kilogram of soil to estimate the nutrient concentration of one million kilograms or more. Areas between sample points are assumed to form a gradient of values, but when soil between original points is tested it seldom follows that assumption (Hedoin et al., 2007). Furthermore, Virginia P fertilizer recommendations for maize (*Zea mays* L.) are based on soil test response categories developed more than 20 years ago (Donohue & Heckendorn, 1994) and may not accurately reflect yield response of modern crop hybrids. Inconsistent yield response to fertilization based on soil test phosphorus (STP) levels in soybean (*Glycine max* [L.] Merr.) and maize (Sawyer et al., 2002; Fu et al., 2010) may arise from these potential sources of error and variability.

Variable-rate P fertilization can decrease over-application of fertilizer to phosphorus rich areas of the field, but variability in subsequent crop yield has still occurred (Wittry and Mallarino, 2004; Bermudez and Mallarino 2007). Due to large spatial variability of STP, increasing the resolution of P mapping at field scale (i.e. more samples per hectare) by decreasing the distance between data points can result in more accurate placement of fertilizer (Franzen and Peck, 1995; Mallarino and Wittry, 2004). More precise fertilizer application could simultaneously reduce under-fertilized and over-fertilized zones, benefiting the farmer and the environment. Although increased precision of fertilizer application is desirable, the feasibility of acquiring such data with current soil testing methods is economically impractical for farmers due to the number of required samples per hectare (Grandt et al., 2010).

Costly high-resolution soil sampling beckons the need for new techniques to increase the resolution of soil P data. Spatially mapping plant available phosphorus (PAP) with remotely sensed data collected from phosphate-sensitive plants may provide an economical means of creating P application recommendations. This novel approach of using a cover crop to predict nutrient needs of the subsequent cash crop (i.e. an 'indicator crop') has not yet been presented in the literature. The *Arabidopsis thaliana* mutant '*ipk1*$^{-}$' (Kuo et al., 2014) exhibits an inverse relationship between phosphate levels in growth medium and biomass production, and therefore may be a strong indicator crop proof-of-concept candidate to test PAP response at P concentrations mimicking the range of STP used for maize fertilizer recommendations in Virginia.

The goal of this project was therefore to determine whether utilizing remotely sensed plant response data to estimate plant available phosphorus could provide a precise and cost-effective spatial phosphorus map. Fractional green canopy cover has been shown to correlate with leaf area index, normalized difference vegetation index, and aboveground plant biomass (Carlson and Ripley, 1997; Lati et al., 2011; Nielsen et al., 2012), making FGCC a practical tool for estimating biomass of potted plants compared to large-scale methods (e.g. satellite remote sensing). Therefore, our objective was to determine whether growth (i.e. fractional green canopy cover [FGCC] derived from the application Canopeo® [Oklahoma State University, Stillwater, Oklahoma]) of the *ipk1*$^{-}$ mutant correlated to media phosphorus concentrations similar to those used for fertilizer decision making in the field.

METHODS

Arabidopsis thaliana Inositol Phosphate Kinase 1 loss-of-function mutant (*ipk1*$^{-}$) was seeded in a factorial design of three seeding rates by nine soil phosphorus rates and replicated three times. Potassium phosphate (KH_2PO_4) was added to deionized water to form concentrations of 0, 5, 10, 15, 25, 30, 40, 50, and 60 mg kg^{-1} P to mimic maize soil test P levels for Virginia using Mehlich-1 extraction (Table 3.1). Vermiculite was saturated using each P concentration solution and then added to 7-cm square pots (n = 3 replicates per treatment). Seeds were sown at 3 mm depth in each vermiculite P concentration at 4, 8, or 12 seeds per pot, with two seeds placed at each location (Figure 3.1) to later be thinned to one plant per location if both seeds germinated. Pots were placed in trays in a growth chamber set to 16-hour day length at 150 μE m^{-2} s^{-1} light intensity, 21°C air temperature, and 55% humidity. Trays were watered as necessary with a solution of deionized water and a ¼ rate of the macro- and micronutrient solution developed by Murashige and Skoog (1962) and rotated periodically to mitigate potential edge-effects from growth chamber variability. *Arabidopsis* was thinned to one plant per seeding location (where necessary) 14 days after seeding. Pots were placed below a stationary Samsung Galaxy Note 8© camera 30 days after planting for consistent imaging of each pot. Images were cropped to a square covering twice the area of the soil surface to encompass leaves extending past pot edges (Figure 3.2A). The application Canopeo© was used to quantify FGCC for each image (Figure 3.2B) as described by Patrignani and Ochsner (2015). Aboveground plant biomass was harvested after imaging on a per-pot basis and number of live plants per pot was recorded. Average leaf area per plant was calculated by dividing the FGCC per pot by the number of plants harvested from the corresponding pot and multiplying the quotient by the total area (in cm^2) represented in each image. Average biomass per plant was calculated by dividing the total biomass per pot by the number of plants harvested from the corresponding pot. Data in this study were adjusted to a per-plant basis where applicable to mitigate for missing plants by multiplying the per-plant biomass and leaf area by the number of missing plants and adding the product to the total biomass or leaf area per pot, respectively. Plant tissue collected from each pot was placed in a forced air drier at 60°C for 24 hours and promptly weighed. Relationships between biomass, leaf area, and media P concentrations were analyzed using linear regression in JMP® Pro 14 (SAS Institute, 2018) using α = 0.05. Analysis of variance (ANOVA) was conducted using JMP for plant germination data. Replication was treated as a random factor. When a significant *F* value was detected by ANOVA at $\alpha = 0.05$ treatment means were separated using Fisher's protected LSD.

RESULTS AND DISCUSSION

Germination

Although not statistically significant ($p = .17$), a trend to have decreased germination at very low (i.e. 0 and 5 mg kg^{-1}) P concentration seemed to occur (Table 3.2). Since two seeds were placed at each seeding location, lack of a plant represents the failure of both seeds to germinate. Although 0 mg kg^{-1} P is unlikely in an agricultural field, 5 mg kg^{-1} P is possible in areas of poor soil fertility. The *ipk1*$^{-}$ mutant was reported to uptake more P than wild-type *Arabidopsis thaliana* (Kuo et al., 2014), so failure to germinate at 5 mg kg^{-1} P was not expected. Decreased plant population due to germination failure could under-represent canopy cover measurements made with remote sensing instruments, resulting in decreased P concentration estimation via an indicator crop.

Comparing Leaf Area to Biomass

Strong correlation (r^2 = .96) between aboveground plant biomass per pot and Canopeo fractional green canopy cover values (used to calculate plant leaf area per pot) occurred across all P concentrations tested (Figure 3.3). Variation in linear r^2 and RMSE values was minimal between plant densities (Table 3.3). A large decrease in r^2 value and increase in RMSE would indicate a plateau from saturated groundcover, which was not observed within the plant densities tested. Leaf area plateau could result from bolting (i.e. the production of a flowering stem) or plant leaves overlapping (Figure 3.5). Bolting in *Arabidopsis* (Figure 3.5A) was not consistent within pots but tended to occur most frequently in larger plants. Bolting is not a desirable characteristic for the methods of indicator crop implementation in this study due to the resulting skew of biomass to green area. Relatively tall stalks and flowers can add biomass, while only slightly increasing, or even decreasing, green area due to the perpendicular nature of stalks compared to sensors and the color of flowers being outside the green spectrum. Figure 3.5B shows a plant leaf overlapping another leaf on the same plant (“self-overlap”), which can occur at any plant density and is more likely with larger plants. Similar to bolting, self-overlap can result in decreased observed leaf area regardless of plant population. However, “cross-overlap” (i.e. when the leaf of one plant obstructs the view of another plant’s leaf; Figure 3.5C) is more likely to occur both with large plants *and* at greater plant density. Cross-overlap could result in a less linear relationship between leaf area and biomass at increasing plant density since plants are placed more closely together and therefore leaf area is more likely to become saturated at greater plant biomass.

Response to Media P Concentration

Measured leaf area response to media P concentration varied based on whether pots contained two, four, or six plants per pot (Figures 3.6A, 3.6B, and 3.6C, respectively). All plant populations exhibited the expected response to increasing P concentration (i.e. decreased growth), but not until P concentrations exceeded the regression curve maxima of 35.7, 37.3, and 38.1 mg kg^{-1} for two, four, and six plants per pot, respectively. Increased plant density (i.e. 6 plants pot^{-1}) resulted in greater correlation between leaf area and P concentration (r^2 = .89) because more plants per pot corresponded with less variability between replications. The quadratic growth response of the *ipk1⁻ Arabidopsis* mutant in this test would not be conducive for fertilizer recommendations to fields with unknown soil P concentrations since it would not be possible to discern between the leaf area corresponding to the left or right of the curve maximum. However, some insight could be gained if soil data approximate values were known. For example, at the six plants per pot plant density, an average leaf area above 8 cm^2 would represent P concentrations between 15 and 60 mg kg^{-1} (Figure 3.6C). Altering the response curve though genetic manipulation of this mutant or investigating other P-sensitive mutants could result in an indicator suitable for a wider range of field P scenarios. By shifting the curve maximum to 60 mg kg^{-1} P, for example, it may be possible to decide between fertilizing or not fertilizing in agricultural fields containing 5

– 100 mg kg^{-1} P; this hypothetical growth response could increase the application of this strategy to a wider range of fields.

Alternatively, future iterations of indicator crop development could seek alternate methods to show variations in soil nutrient levels. Change in leaf color, for example, could be detected with remote sensing on a relatively small grid size and show a gradient in soil nutrient level without sacrificing cover crop biomass. Development of such a trait should then be transferred to a crop more easily planted in an agricultural field. Work with field pennycress (*Thlaspi arvense* L.) is already underway at Virginia Tech due to its genetic similarity to *Arabidopsis* (Chopra et al., 2018), larger seeds for ease of sowing with equipment, and relative hardiness outdoors (McGinn et al., 2019).

CONCLUSIONS

Leaf area per plant exhibited a strong quadratic relationship (r^2 = .89 for 6 plants pot^{-1}) with media P concentration. Increased *ipk1*⁻ plant density helped mitigate occasional outliers in plant size and resulted in greater r^2 values between average plant leaf area and P concentration, indicating that 6 plants pot^{-1} was the optimal plant density in this study. The very strong correlations between leaf area and aboveground biomass (r^2 = .96) suggests the plant structure of *Arabidopsis* is well suited for a biomass-responsive indicator crop. Maximum plant leaf area occurred between 36 and 38 mg kg^{-1} P regardless of plant density (2, 4, or 6 plants pot^{-1}), which is within the range of agronomic decision making. While strong correlations between plant leaf area and soil nutrient level imply a promising approach to plant available nutrient mapping, mutants with a different response to P concentration may be required in fields with high variability in soil P levels. Further research is also warranted to compare indicator crop response in the field to yield response in the subsequent cash crop to determine whether measured plant available P produces more consistent response to P fertilization.

Table 3.1. Maize soil test P levels and corresponding soil test P concentrations developed for Virginia (Maguire and Heckendorn, 2019).

Maize P Level	Soil P concentration mg kg^{-1}
Low -	0–2
Low	2–4
Low +	5–6
Medium -	6–10
Medium	11–15
Medium +	16–18
High -	18–28
High	28–43
High +	43–55
Very High	55+

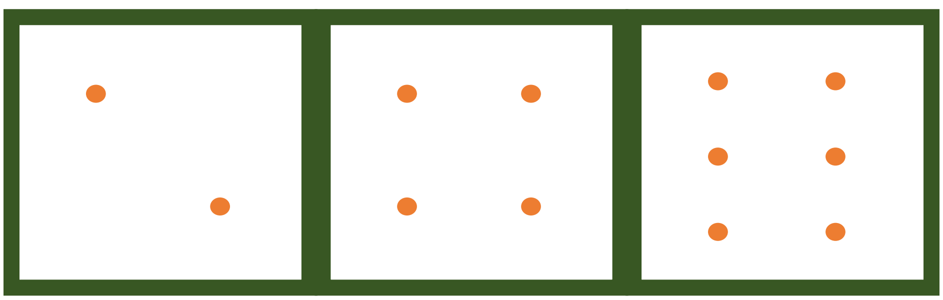

Figure 3.1. Orange dots representing seeding locations within pots.

Figure 3.2. A cropped image before (A) and after (B) Canopeo green pixel identification.

Table 3.2. Missing plants for each P concentration across three seeding rates (4, 8, and 12 seeds per pot, seeded in duplicate at 2, 4, and 6 locations per pot, respectively). A missing plant represents failure of both seeds at a seeding location to germinate, i.e. germination rate was less than or equal to 100 – the percentage of missing plants. Values followed by the same letter within location are not significantly different at α=0.05.

P concentration mg kg^{-1}	Missing plants %	
0	13	a
5	18	a
10	4	a
15	0	a
25	2	a
30	0	a
40	7	a
50	6	a
60	6	a

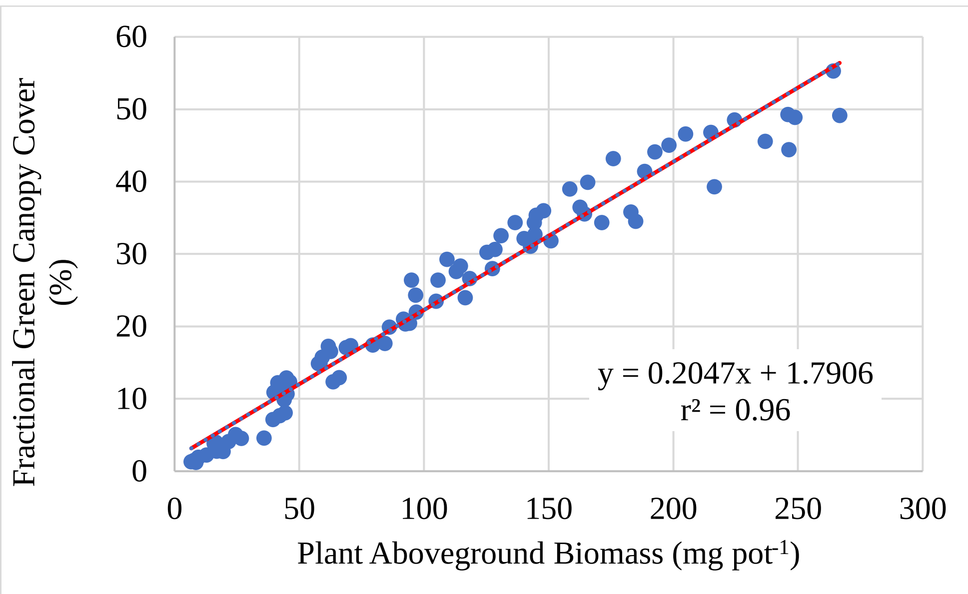

Figure 3.3. The relationship between fractional green canopy cover reported from Canopeo and dry biomass per pot across all P concentrations tested.

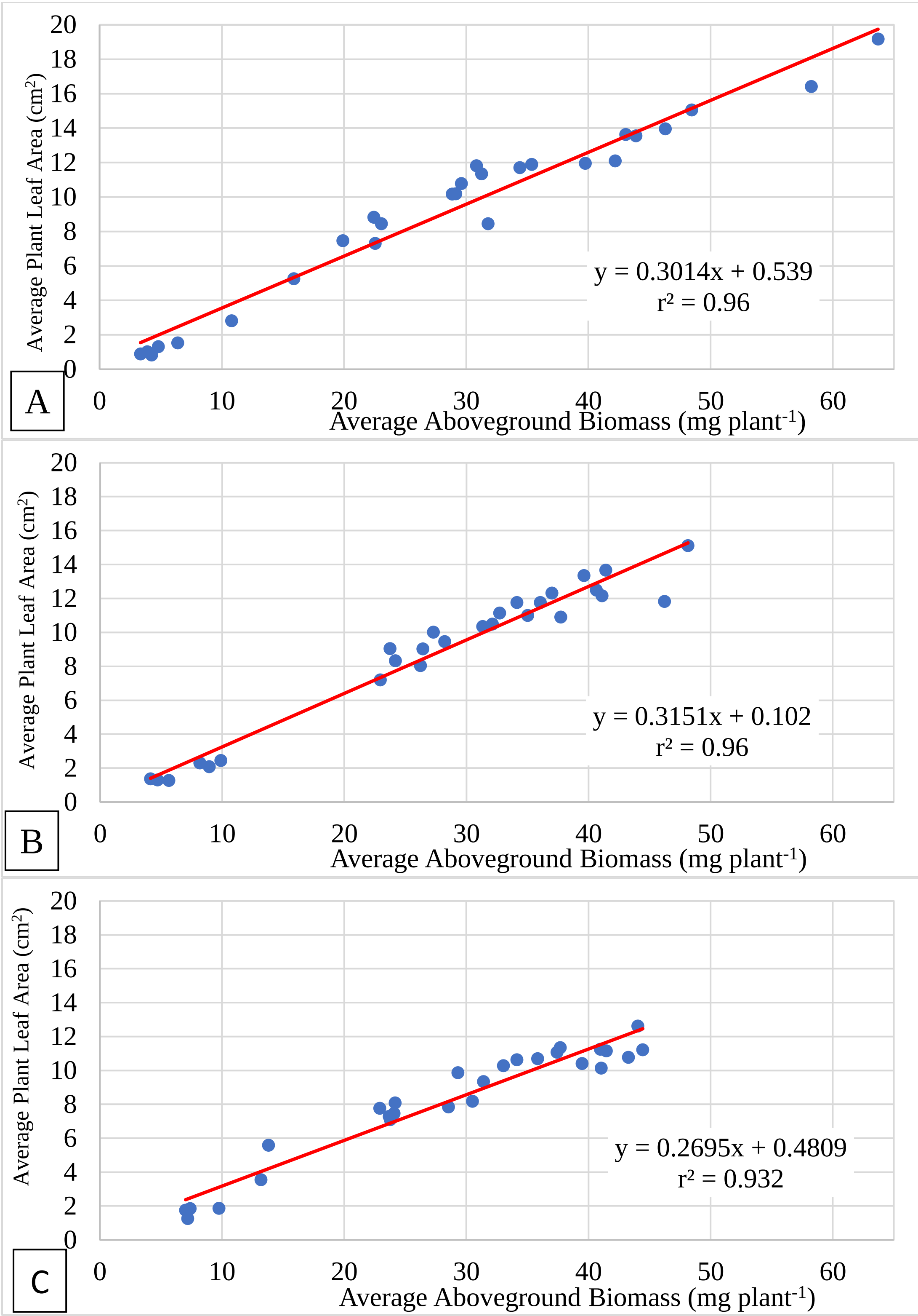

Figure 3.4. The relationship between leaf area per plant and average aboveground biomass for plant densities of 2 (A), 4 (B), and 6 (C) plants per pot ($P > F$ = <0.0001 for each plant density).

Table 3.3. Comparison of plant leaf area and biomass for two, four, and six *Arabidopsis* plants per 75 cm^2 pot.

	Plants per pot		
	2	4	6
r^2	0.96	0.96	0.93
RMSE	1.03	0.89	0.91
Prob > F	<.0001	<.0001	<.0001

Figure 3.5. Potential causes of increased biomass to leaf area ratio. A) Bolting, or the production of a flowering stem. B) A plant leaf overlapping another leaf on the same plant (self-overlap). C) A plant leaf overlapping the leaf of another plant (cross-overlap).

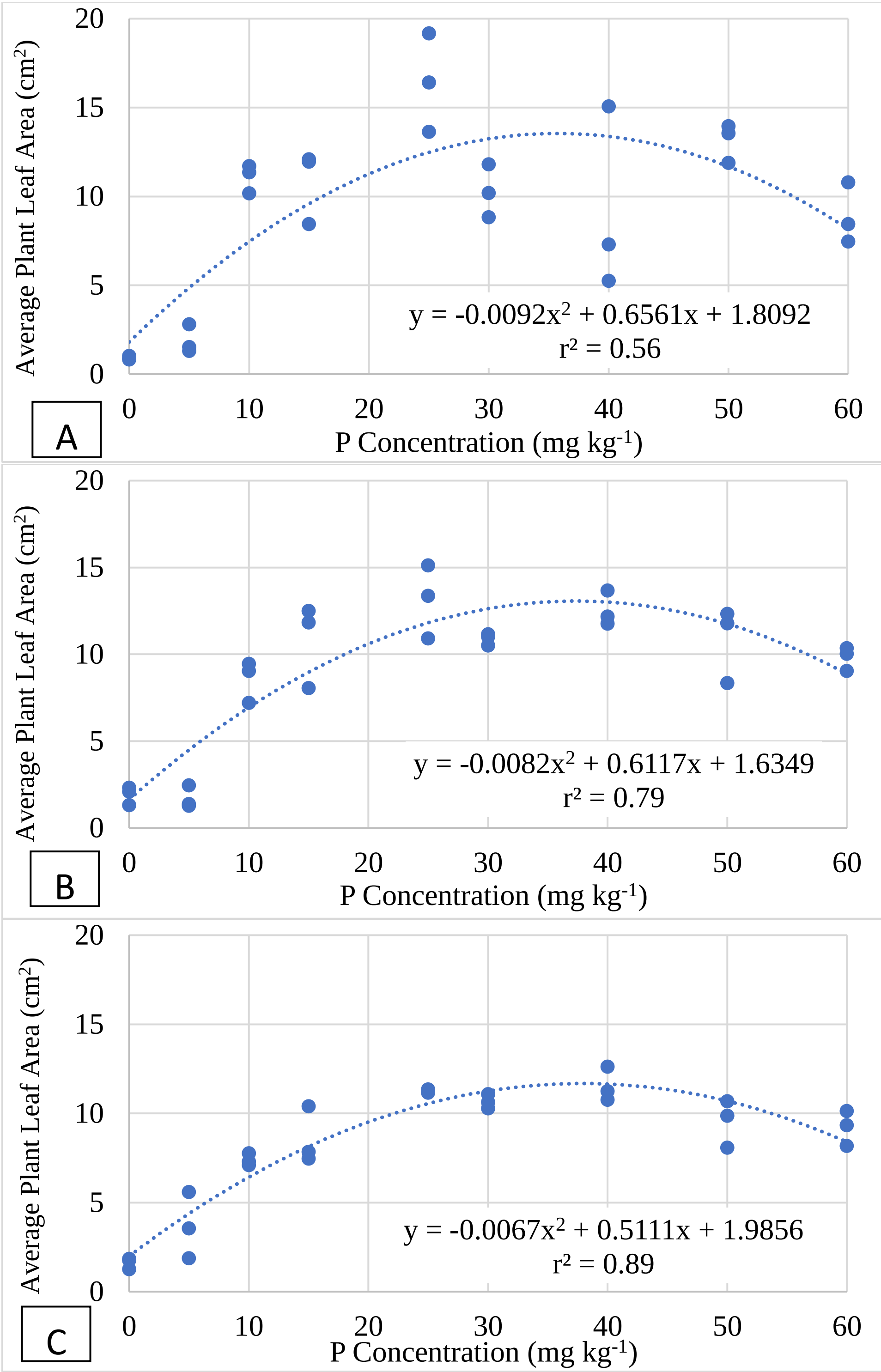

Figure 3.6. The relationship between mutant green area per plant and soil P concentration for plant densities of 2 (A), 4 (B), and 6 (C) plants per pot ($P>F$ = <0.0001 for each plant density). Blue dots represent the Canopeo value per pot divided by the number of plants in that pot for *ipk1⁻* at each soil P concentration. The equation for each trendline is shown within its respective graph.

BIBLIOGRAPHY

Bermudez, M. & Mallarino, A. P. 2007. Impacts of variable-rate phosphorus fertilization based on dense grid soil sampling on soil-test phosphorus and grain yield of corn and soybean. Agronomy Journal, 99, 822-832.

Carlson, T. N. & Ripley, D. A. 1997. On the relation between NDVI, fractional vegetation cover, and leaf area index. Remote sensing of Environment, 62, 241-252.

Chopra, R., Johnson, E. B., Daniels, E., Mcginn, M., Dorn, K. M., Esfahanian, M., Folstad, N., Amundson, K., Altendorf, K. & Betts, K. 2018. Translational genomics using Arabidopsis as a model enables the characterization of pennycress genes through forward and reverse genetics. The Plant Journal, 96, 1093-1105.

Donohue, S. & Heckendorn, S. 1994. Soil test recommendations for Virginia. Virginia Cooperative Extension Service Publ, 834, 23-27.

Franzen, D. W. & Peck, T. R. 1995. Field soil sampling density for variable rate fertilization. Journal of Production Agriculture, 8, 568-574.

Fu, W., Tunney, H. & Zhang, C. 2010. Spatial variation of soil test phosphorus in a long-term grazed experimental grassland field. Journal of Plant Nutrition and Soil Science, 173, 323-331.

Grandt, S., Ketterings, Q. M., Lembo, A. J. & Vermeylen, F. 2010. In-field variability of soil test phosphorus and implications for agronomic and environmental phosphorus management. Soil Science Society of America Journal, 74, 1800-1807.

Grunwald, S., Reddy, K. R., Newman, S. & Debusk, W. F. 2004. Spatial variability, distribution and uncertainty assessment of soil phosphorus in a south Florida wetland. Environmetrics, 15, 811-825.

Kuo, H. F., Chang, T. Y., Chiang, S. F., Wang, W. D., Charng, Y. Y. & Chiou, T. J. 2014. Arabidopsis inositol pentakisphosphate 2-kinase, A t IPK 1, is required for growth and modulates phosphate homeostasis at the transcriptional level. The Plant Journal, 80, 503-515.

Lati, R. N., Filin, S. & Eizenberg, H. 2011. Robust methods for measurement of leaf-cover area and biomass from image data. Weed Science, 59, 276-284.

Maguire, R. & Heckendorn, S. 2019. Soil test recommendations for Virginia. Virginia Cooperative Extension, -.

Mallarino, A. P., Sawyer, J. E. & Barnhart, S. K. 2013. A general guide for crop nutrient and limestone recommendations in Iowa.

Mallarino, A. P. & Wittry, D. J. 2004. Efficacy of grid and zone soil sampling approaches for site-specific assessment of phosphorus, potassium, pH, and organic matter. Precision Agriculture, 5, 131-144.

Mcginn, M., Phippen, W. B., Chopra, R., Bansal, S., Jarvis, B. A., Phippen, M. E., Dorn, K. M., Esfahanian, M., Nazarenus, T. J. & Cahoon, E. B. 2019. Molecular tools enabling pennycress (Thlaspi arvense) as a model plant and oilseed cash cover crop. Plant biotechnology journal, 17, 776-788.

Murashige, T. & Skoog, F. 1962. A revised medium for rapid growth and bio assays with tobacco tissue cultures. Physiologia plantarum, 15, 473-497.

Nielsen, D. C., Miceli-Garcia, J. J. & Lyon, D. J. 2012. Canopy cover and leaf area index relationships for wheat, triticale, and corn. Agronomy journal, 104, 1569-1573.

Patrignani, A. & Ochsner, T. E. 2015. Canopeo: A powerful new tool for measuring fractional green canopy cover. Agronomy Journal, 107, 2312-2320.

Preedy, N., Mctiernan, K., Matthews, R., Heathwaite, L. & Haygarth, P. 2001. Rapid incidental phosphorus transfers from grassland. Journal of Environmental Quality, 30, 2105-2112.

Swoish, M. J., Thomason, W., Reiter, M. 2020. Technological Innovations for Mid-Atlantic Cropping Systems. A Dissertation Submitted to Virginia Polytechnic and State University. Chapter 2.

Tiessen, H., Ballester, M. V. & Salcedo, I. 2011. Phosphorus and global change. Phosphorus in action. Springer.

Todd, P. A., Ong, X. & Chou, L. M. 2010. Impacts of pollution on marine life in Southeast Asia. Biodiversity and Conservation, 19, 1063-1082.

Wittry, D. J. & Mallarino, A. P. 2004. Comparison of uniform-and variable-rate phosphorus fertilization for corn--soybean rotations. Agronomy Journal, 96, 26-33.

Conclusions:

Chapter 1 showed that trinexapac-ethyl applied to barley decreased plant height similarly across two common malting barley cultivars grown in Virginia, US. In general, increased application rate and later application timing resulted in shorter plants. Lodging was also significantly decreased in one site-year with any application, although lodging occurrence was minimal even in untreated plants. Grain yield, moisture, and protein were unaffected by application in 2018. However, 2019 revealed that significant plant injury and yield reduction could occur if trinexapac-ethyl application was preceded by cool weather and followed by warm weather. Decreased wheat yield was present in the literature, though rare, and decreased malt barley yield had not been reported. Plant growth regulators are a means to mitigate risk of lodging, but the risk of yield loss observed in this study indicates trinexapac-ethyl should be used with caution for malt barley in warm weather. Application is not advised unless lodging risk is elevated (e.g. cultivars with greater average plant height and/or weaker stems). Further research is warranted on cultivars more prone to lodging.

Chapter 2 proved that satellite imagery could accurately predict biomass of mixed-species cover crops, although vegetation index (VI) selection was important and varied by satellite. Perpendicular vegetation index was the most accurate VI for Landsat 8 and Planet, whereas ratio vegetation index was most accurate for Sentinel 2. Normalized difference vegetation index, the most widely published VI for biomass estimation, did not perform as well as the aforementioned VIs. Biomass estimation accuracy increased overall when data were averaged across all sites within an agricultural field, which may be beneficial for large-scale estimation of biomass (i.e. estimating average growth across a watershed). The for-pay satellite imagery from Planet did not estimate biomass as accurately as Landsat 8 or Sentinel 2 (both of which offer free imagery) across most VIs. However, inherent advantages of increased spatial and temporal resolution such as clearer imagery and image availability for every site, respectively, indicated usefulness of this new technology for agricultural purposes. Further research should increase the number and breadth of in-field cover crop samples to expand the amount of data to compare to VIs across satellite imagery. With further analysis, satellite imagery could help implement a performance-based cover crop payment program.

Chapter 3 showed the promise of an indicator plant for estimating plant available phosphorus across an agricultural field at high spatial resolution. The *ipk1*$^{-}$ *Arabidopsis* mutant exhibited a very strong relationship between plant leaf area and media phosphorus concentration. Leaf area was also highly correlated to biomass, indicating methods like those in Chapter 2 may be useful for estimating phosphorus concentration across an agricultural field. Further research is warranted on plants that are similar to *Arabidopsis* genetically, but more feasible for cover crop implementation (e.g. field pennycress). If field trials displayed similar plant response to available phosphorus then this technology could result in a more precise, and potentially more accurate, method of nutrient level identification for subsequent variable-rate fertilizer application.

Innovation and adoption of technology for agricultural production in necessary to continue meeting the food, fuel, and fiber requirements of the world. Research projects like those summarized above will be crucial to completing this mission. Further steps should be taken to validate and expand upon the results presented in this dissertation.